

## Review article

## A review of porous electrode structural parameters and optimization for redox flow batteries

Pengfei Wang<sup>a,b</sup>, Yijian Zhao<sup>a,b</sup>, Yuhang Ban<sup>b</sup>, Menglian Zheng<sup>a,b,c,\*</sup><sup>a</sup> State Key Laboratory of Clean Energy Utilization, Zhejiang University, Hangzhou 310027, China<sup>b</sup> Institute of Thermal Science and Power Systems, School of Energy Engineering, Zhejiang University, Hangzhou 310027, China<sup>c</sup> Institute of Wenzhou, Zhejiang University, Wenzhou 325036, China

## ARTICLE INFO

## Keywords:

Redox flow battery  
Carbon electrode  
Electrode parameters  
Mass transfer  
Specific surface area

## ABSTRACT

Redox flow batteries (RFBs) have emerged as promising and highly scalable technologies for durable energy storage systems. The porous electrode, as a vital component facilitating redox reactions, plays a crucial role in maintaining high battery performance. The microstructure of commonly employed porous electrodes is characterized by complexity and stochasticity, which make the process of ion and electron transport inside the electrode difficult to understand. This comprehensive review aims to present a thorough examination of the influences of various microstructures, including specific surface area, porosity, pore size, fiber diameter, pore morphology, and functional groups on the performance of RFBs. The contradiction between permeability and specific surface area is mainly considered and discussed. Moreover, recent advancements in optimizing microstructure for porous electrodes are critically assessed. The review also encompasses an in-depth discussion on advanced characterization methods and manufacturing techniques for higher performance electrode preparation. This review seeks to provide a reference for researchers to optimize the performance of porous electrodes according to the microstructure in RFBs.

## Nomenclature

RFB	redox flow battery
ECSA	electrochemically active specific surface area
EDLC	electric double-layer capacitor
ECF	electrospinning carbon fiber
AECF	aligned electrospinning carbon fiber
MIP	mercury intrusion porosimetry
BET	Brunauer-Emmet-Teller methods
DPCE	dual-scale porous electrode
SF	shape factor
CT/XCT	X-ray transmission computed tomography
LBM	Lattice-Boltzmann Method
$\kappa$	local permeability
$d_f$	fiber diameter
$d_p$	pore diameter
$\epsilon$	porosity
$K_{CK}$	Carman-Kozeny constant
$a$	specific surface area
$V$	volume of pores

$S$	specific surface area of pores channel
$\tau$	tortuosity
$u$	velocity

## 1. Introduction

Energy is the backbone of the modern society. With the global energy demand rising each year, the proportion of renewable energy is also increasing. However, the intermittency and volatility of renewable energy generation have led to a mismatch between energy supply and demand. To address this challenge, energy storage has become an integral part of energy utilization. Redox flow batteries (RFBs) have emerged as one of the most promising energy storage technologies due to their high safety, stable operation, independent power operation, battery capacity, high energy efficiency, and long battery life [1,2]. They can be used for peak shaving and filling valleys in conventional power grids to improve the grid's stability and security [3,4].

Despite their promising attributes, RFBs face a notable challenge in their relatively low power density [2]. This limitation results in the need for larger-sized systems and a higher number of stacks to achieve large-

\* Corresponding author at: State Key Laboratory of Clean Energy Utilization, Zhejiang University, Hangzhou 310027, China.

E-mail address: [menglian\\_zheng@zju.edu.cn](mailto:menglian_zheng@zju.edu.cn) (M. Zheng).<https://doi.org/10.1016/j.est.2024.112859>

Received 18 March 2024; Received in revised form 20 May 2024; Accepted 7 July 2024

Available online 13 July 2024

2352-152X/© 2024 Elsevier Ltd. All rights reserved, including those for text and data mining, AI training, and similar technologies.

scale energy storage, consequently increasing the overall footprint of the energy storage installations [5]. Therefore, enhancing the power density of RFBs becomes imperative to mitigate investment costs and minimize the required footprint for these energy storage systems. In RFBs, electrochemical reactions take place within the porous electrodes, which are in direct contact with the electrolyte. The porous electrode serves as both the site for the electrochemical reaction and the pathway for the transportation of reactants, products, and electrons [6,7]. The porous electrode greatly affects the power density and other performance of the battery. Carbon felts, carbon cloth, carbon paper, and other carbon-based materials are the commonly used porous electrodes in flow batteries [8]. Currently, carbon felt is the predominant electrode material utilized in flow batteries, recognized for its extensive voltage range, remarkable stability, and economic efficiency. Researchers have focused on modifying carbon felt to augment its electrochemical activity, which is a pivotal area of study within the field [9,10]. The progression of flow battery technology has seen the exploration of diverse carbon materials aimed at enhancing electrode performance. Carbon cloth, characterized by its multi-scaled pores and robust woven structure, presents superior mechanical attributes and has been shown to potentially outperform both carbon felt and carbon paper under laboratory conditions [11]. The unique zero-gap structure of batteries using carbon paper has demonstrated exceptionally high power densities, a benefit derived from the low ohmic resistance of the thin carbon paper [8]. Nonetheless, the suboptimal mechanical strength and hydraulic permeability associated with carbon paper have impeded its widespread adoption. As a result, despite the unique advantages presented by various carbon materials, carbon felt, particularly that synthesized from polyacrylonitrile, has emerged as the leading choice for electrode materials in the commercial sector of flow battery applications. The microstructure of porous

electrodes spans multiple scales, which has an important and complex influence on the mass transfer process of active ions and electrons inside [12]. This complexity has led numerous researchers to investigate the structure of flow battery electrodes to discern how microstructural features impact performance. These studies are instrumental in the ongoing efforts to optimize electrode microstructures and, by extension, elevate battery performance [13–16]. With the progress of manufacturing technology, some novel electrode structures have been realized by advanced manufacturing technology [17,19,20]. However, most of the previous reviews focused on battery performance and battery scale structural characteristics, the current research about microstructure is relatively scattered and lacks systematic sorting and summary. Advanced manufacturing technology needs an in-depth understanding of electrode microstructure to guide the manufacturing of new structures. To guide the design of electrode microstructures, necessary characterization and testing must also be conducted. Current conventional characterization methods include the assessment of both the physical and electrochemical properties of the electrodes. The physical characterization encompasses the measurement of geometric properties such as specific surface area, porosity, and other morphological attributes. Electrochemical characterization, on the other hand, involves the assessment of parameters like charge transfer impedance, diffusion impedance, and electrochemically active surface area (ECSA). However, these characterization techniques are predominantly applied at the battery scale and lack measurements at the local electrode level, which limits their ability to provide guidance for the design of electrode structures.

Herein, this review aims to summarize the key parameters of porous electrode microstructure and their mechanism on the performance of RFBs. By summarizing these contents, it provides guidance for the

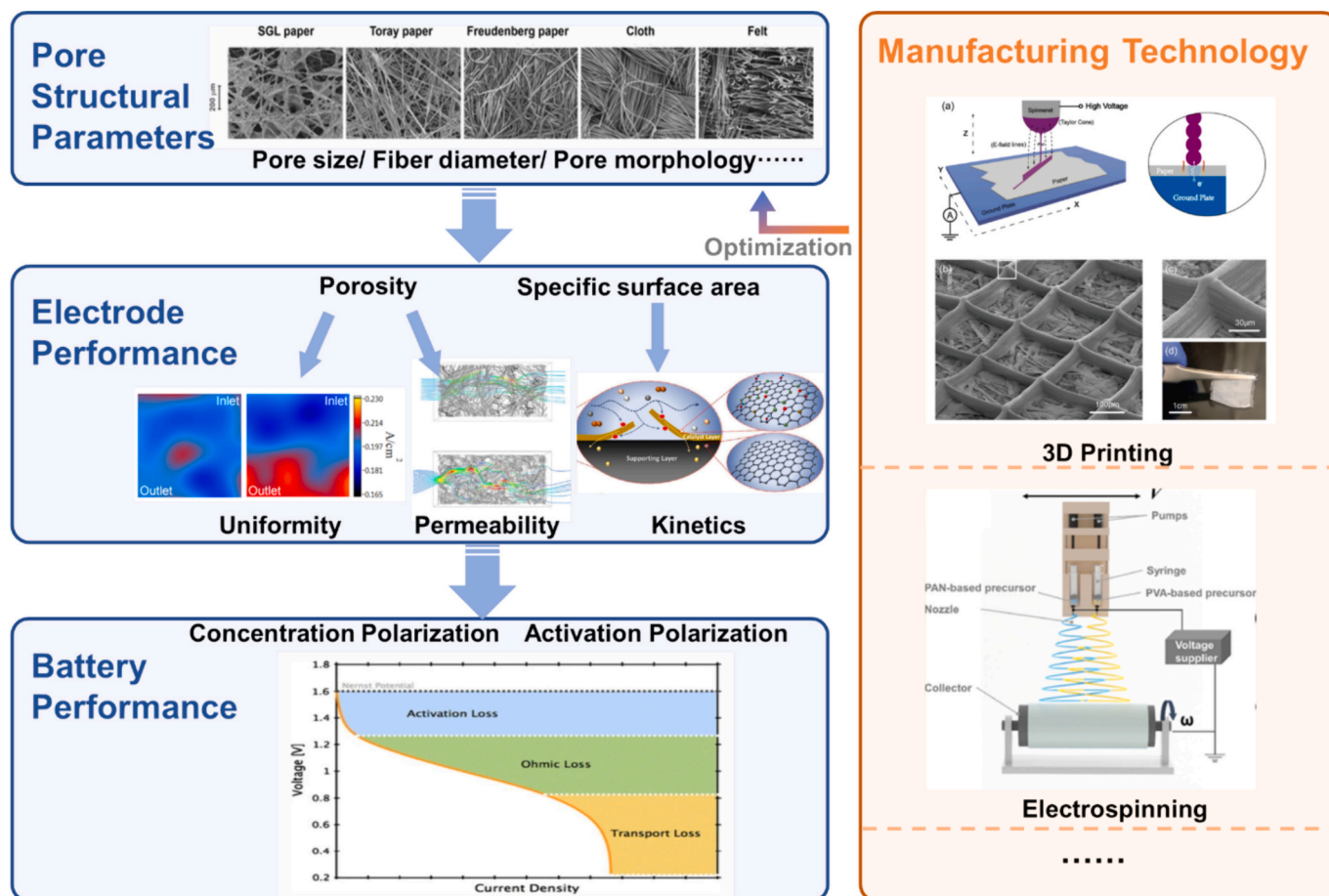


Fig. 1. Effect of porous electrode pore structure on battery performance. Adapted with permission from Ref. [11, 18, 21, 22, 23, 25, 26].

structural optimization of porous electrodes. Additionally, it will outline the latest research progress on optimizing the porous electrode structure, as well as the advanced manufacturing and testing methods for pore-scale optimization (Fig. 1). It is hoped that this review will provide researchers with a valuable reference for subsequent studies.

## 2. Effects of microstructure on electrode performance

In recent years, the manufacturing processes for the commonly used carbon electrodes have been relatively mature. The traditional processes for preparing carbon-based porous electrodes include dip coating [27], doctor blade coating [28], screen printing [29], masking [30], spraying [31], and roll-to-roll printing [32], etc. With the further improvement of technology, some new manufacturing processes have also been applied to prepare electrode materials, such as 3D printing and electrospinning [17,18,20,21,33,34,36].

Generally, the carbon fiber selected for carbon paper can be polyacrylonitrile-based, pitch-based, or cellulose-based carbon fibers. After being immersed in the dispersant solution, the carbon fibers are processed into carbon paper precursor. The carbon fibers of the precursor have large gaps and weak mechanical strength. It is necessary to add resin to increase its mechanical strength. Then carbon paper can be obtained after being cured, molded, carbonized, and graphitized. The carbon paper obtained by this method is composed of random short fibers and is isotropic. However, it is too rigid to bend. It is easy to be damaged during the process of being made into electrodes [37,38].

In the preparation of woven electrodes, long carbon fibers are woven into cloth. Alternatively, the precursor of carbon fibers is woven into a fabric and then carbonized to form carbon cloth. There is no connection between the carbon fibers, so the carbon fibers are not firmly bonded to each other. Some researchers apply phenolic resin on the surface of the carbon cloth and perform a high-temperature carbonization process. By applying a phenolic coating, the carbon fibers can be tightly bonded together to enhance the mechanical strength and stability of the carbon cloth, making carbon cloth more durable and able to withstand large tensile and compressive forces [39,40].

The geometry and morphology of porous electrodes can be characterized by microstructure, such as fiber diameter, pore size, and fiber morphology, and comprehensive parameters affected by microstructural parameters, including porosity, specific surface area, etc. (Fig. 2). Herein, we briefly review the effects of the microstructure on the performance of porous electrodes to gain a better understanding of the

mechanisms of the electrode's parameters on RFB's performance and to provide some guiding opinions on the desirable microstructure of novel porous electrodes (Table 1).

### 2.1. Porosity

Porosity is one of the most commonly used characteristic parameters of porous electrodes. It represents the proportion of the pore phase in the porous electrode. This is mutually dependent on the surface area of the non-porous phase. Generally, an increment in the porosity leads to a reduced specific surface area while an enhancement in the permeability for a smooth surface carbon fiber electrode. In the field of porous media, many models have been proposed to investigate the relationship between permeability and porosity. However, the results of different models vary greatly. There may be an order of magnitude difference in permeability at a given porosity. Ke et al. believed that this gap might be caused by the fact that some models were based on Archie's law which was calculated by the resistivity of porous media to obtain permeability, while other models were based on Darcy's Law [41]. Even models that are also based on Darcy's Law differ somewhat. This may be because different models are based on different assumptions about microstructure. For example, the Carman-Kozeny equation mainly assumes spherical particles and does not consider the contact area between particles. Some other models, such as Tamayol-Bahrami model and Doormaal-Pharoah model, assume that porous media are fibers in contact with each other. In the field of porous electrodes, the most commonly used model is Carmen-Kozeny equation.

$$\kappa = \frac{d_f^2 \epsilon^3}{K_{CK}(1 - \epsilon)^2} \tag{1}$$

**Table 1**  
Main microstructure parameters of porous electrode.

Parameter	Definition
Porosity	Proportion of pore phase volume to total volume
Specific surface area	Internal surface area per unit mass of a porous solid substance
Pore size	Diameter of internal pores of a porous material
Fiber diameter	Diameter of fiber cross-section
Tortuosity	Ratio of actual path length to the shortest path from the starting point to the endpoint of flow

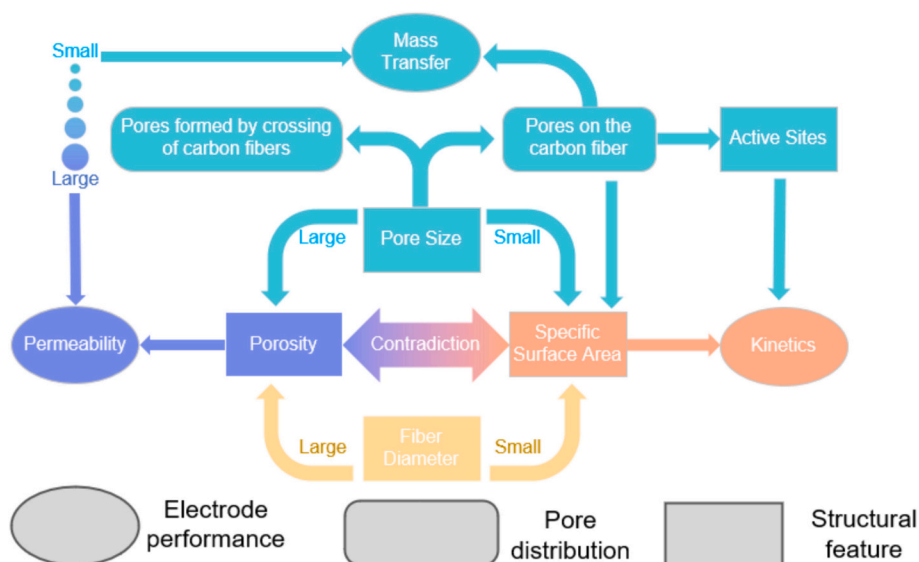


Fig. 2. Schematic of effects of microstructure parameters on electrode performance.

where  $\kappa$  is the local permeability,  $d_f$  is the fiber diameter,  $\varepsilon$  is the porosity, and  $K_{CK}$  is the Carman-Kozeny constant. The reliability and adaptability of this equation have also been considered by many researchers. Gostick et al. measured the in-plane and through-plane permeability of carbon fiber materials with different porosity. They compared the relationship between permeability and porosity with common models. The experimental results match well with Tomadakis and Sotirchos' model, which was developed from Carman-Kozeny equation [42]. So far, the Carman-Kozeny equation has been modified to improve the accuracy of the calculation.  $K_{CK}$  is an empirical constant, and there are usually two ways to estimate it. Some researchers substituted  $K_{CK}$  into the equation as a constant. According to different types of porous media, researchers used experimental or simulation methods to deduce the value of  $K_{CK}$  for different microstructures. Li et al. experimentally determined that the  $K_{CK}$  value in porous fiber was 12.81 [43]. Another group of researchers treated  $K_{CK}$  as a function of pore structural parameters. Pacella et al. experimentally measured the permeability of hollow fiber bundles at a certain porosity. The linear relationship between  $K_{CK}$  value and porosity was established in this study [44]. Liu et al. used finite element analysis to conduct numerical simulations of fiber structure. They explored material permeability under different fiber arrangements and established the relationship between  $K_{CK}$  and fiber volume fraction [45]. Using the modified Carman-Kozeny equation, the researchers made more accurate predictions of the permeability of the porous electrode.

## 2.2. Specific surface area

The surface of carbon fibers is the place where a redox reaction occurs. The larger the specific surface area is, the more active sites for the reaction to occur. Usually, the specific surface area is characterized by using the BET and the MIP methods. Both methods work by applying pressure that causes gas or mercury to penetrate the porous material. However, BET cannot measure the distribution of large pores (>50 nm) and MIP cannot measure the distribution of micro pores (<5 nm) due to the limitation of the applied pressure intensity. Alternatively, the specific surface area can be predicted through mathematic models. For example, Carta et al. developed a model that correlated the specific surface area with the porosity and fiber diameters [46].

$$a = \frac{4}{d_f}(1 - \varepsilon) \quad (2)$$

where  $a$  is the specific surface area,  $d_f$  is the fiber diameter, and  $\varepsilon$  is the porosity. However, there is often a difference between the specific surface area predicted by the mathematical model and the actual specific surface area. Weber et al. believed the reason for this difference was that fibers were in contact and overlapped each other [47]. Besides, the shape of fibers also significantly affects the resulting specific surface area, which was not incorporated in the mathematical model. Emmel et al. used X-ray tomography to photograph carbon felts. The authors found that indentation with a depth of approximately 50 nm on the fiber surface significantly increases the specific surface area [14]. Likewise, the presence of a large amount of binders in carbon paper (manufactured by SGL Carbon Inc.) also significantly impacts the prediction of the specific surface area. To be specific, the surface of fibers is not completely smooth, and the bumps or depressions of fibers can significantly change the specific surface area of the resulting porous media.

For the flow battery, the electrolyte interacts with the active site on the electrode surface. Due to the hydrophilicity difference and "dead zones" (no electrolyte flowing through) of the electrode, the electrolyte does not fully reach the entire specific surface area of the porous electrode. In addition to the traditional geometric specific surface area, the electrochemically active specific surface area (ECSA) is more critical for porous electrodes, that is, the area where the active site and the electrolyte are in contact. Since the traditional physical method is

challenging to measure ECSA, it is usually determined according to the electric double layer capacitor (EDLC), which is calculated based on the measured capacitance and the area-specific capacitance. ECSA is generally smaller than that measured by the BET method. The difference between the two can be one or two orders of magnitude, which is due to that the BET method can detect micropores that the electrolyte cannot reach under ambient pressure.

It can be seen that for porous electrodes, higher porosity, and larger specific surface area are often contradictory. To a large extent, the optimal design of electrode microstructure is to achieve a better balance between the two. Researchers often employ various strategies to optimize this relationship, such as using hybrid materials, creating hierarchical pore structures, or modifying the pore size distribution to enhance both SSA and the transport properties of the electrode. For example, according to the type of polarization loss in different regions in the electrode, Chen et al. designed electrodes with variable porosity to balance the concentration polarization and activation polarization to minimize the polarization loss of a whole. The simulation results show that the variable porosity electrode can enhance the uniformity of electrolyte flow, enhance the mass transfer ability, and reduce the concentration polarization compared with the traditional electrode with a fixed porosity [48]. However, this optimization method still cannot realize the full utilization of porous electrodes, so it is still necessary to understand the mechanism of electrode parameters at the pore scale and optimize them.

## 2.3. Pore morphology

Under the same porosity and pore size, the differences in the pore morphology resulting from the different arrangements of carbon fibers also significantly affect the electrochemical performance of the flow battery. First, with respect to the cross-sectional shape of the flow channel formed by the fibers, it is found that the pore shape at the cross-section has an impact on the mass transfer of the electrolyte. Niu et al. studied the effects of the pore morphology on the performance of the solid oxide fuel cells. The authors found that the cross-sectional shape of the pores affects the Knudsen diffusivity. The increase in the length-diameter ratio of the cross-sectional shape would lead to a decrease in diffusivity and, thus, an increase in concentration polarization [15]. Additionally, under the same porosity, the porous material with irregular pores has a larger geometrical specific surface area compared to that with regular pores. Ma et al. introduced a dimensionless parameter, i.e., shape factor (SF), to characterize the shape of pore's cross-section, which was defined as the ratio of the perimeter of the equal-area circle of pore's cross-section to the actual perimeter of the cross section.

$$SF = \frac{d_p}{\left(\frac{V}{S/4}\right)} \quad (3)$$

where  $d_p$  is the pore diameter,  $V$  is the volume of the pore, and  $S$  is the specific surface area of the pore channel. Based on the 2-D simulative results, the authors found that the smaller the SF, the more irregular the shape of the carbon fiber was [49]. In other words, the larger the SF, the larger the specific surface area of the carbon fiber under the same porosity, which would help improve the reaction kinetic performance of the electrode. Although the above discussion on the effects of the pore morphology provides guidance for preparing the microstructure of porous electrodes, there are significant gaps between the investigated idealized cross-sectional shapes of the pores and those formed by carbon fibers. Moreover, carbon fiber electrodes are usually woven from carbon fibers, the flow paths are typically not straight but tortuous. The tortuosity, which is usually characterized through the MIP method, represents the ratio of the actual path length to the shortest path from the starting point to the endpoint of the flow [50]. Duta et al. derived the following expression of tortuosity directly based on the fluid velocity.

$$\tau = \frac{\sum \sqrt{u_x^2 + u_y^2 + u_z^2}}{\sum |u_x|} \quad (4)$$

where  $\tau$  is the tortuosity,  $u$  is velocity, and  $x, y, z$  denotes the direction under consideration [51]. Generally, a high tortuosity reduces the permeability, thereby the mass transfer performance, and increases the pump losses through the elongated flow path of the electrolyte within the porous electrode. Wang et al. compared three different shapes of pore-scale flow paths, i.e., cylindrical, slit, and spherical channels. Through simulations, the authors found that cylindrical pores yielded the minimum tortuosity and highest distribution uniformity of the electrolyte velocity, partly owing to the reduced dead zones in less tortuous pores [52]. Furthermore, a reduction in the tortuosity of pores usually yields a narrowed distribution of pore sizes, thereby enhancing the uniformity of electrolyte flow distribution within the whole electrode. Song et al. investigated the effect of tortuosity on electrochemically active sites in porous carbon materials. Two mesoporous carbon materials (ordered mesoporous carbon and disordered mesoporous carbon) with similar pore structure parameters were compared. The carbon nanotubes inside the ordered mesoporous carbon were arranged regularly, and the mesoporous pores were highly ordered and had good interconnection. Therefore, the ordered mesoporous carbon could enhance the mass transfer ability. Another carbon material with tortuous pore shapes did the opposite [53]. The tortuosity is also affected by the degree of the electrode compression. Jervis et al. found that when the compression ratio exceeded 50 %, every 5 % increase would increase the tortuosity by 6.2 % to 7.6 % [54]. At present, there are few pore-scale works to optimize the pore morphology.

#### 2.4. Pore size

As defined by the International Union of Pure and Applied Chemistry, pores in solid materials can be divided into three categories according to their sizes: micropores (<2 nm), mesopores (2–50 nm), and macropores (>50 nm) [55]. With respect to macropores, the diameter of the pores formed by crossing of carbon fibers typically spans the range from a few hundreds of nanometers to hundreds of micrometers. Generally, it has been largely agreed that larger pores favor the permeability of the porous electrode at the expense of the reduced specific surface area, while smaller pores favor the mass transfer process by reducing the diffusion path of the reactants from the bulk electrolyte to the surface of the fibers. These contradictions can be partly relieved by the bimodal pore structure that combines macropores at two or more distinct sizes. To this end, micropores are typically added to the surface of carbon fibers to enlarge the specific surface area. Mesopores are therefore proposed to be added to bridge micropores and macropores to enhance mass transfer of the reactants when they are transferred from bulk solution to the surface of the fibers. Considering that the pores with

the same pore size will have different effects at different locations, we divide them into two categories according to the location of the pores. For example, the pores of tens to hundreds of nanometers in the fiber gap will limit the permeability of the electrolyte, but when on the fiber surface they will enhance the mass transfer effect of ions. The previous studies on the manufacturing methods for obtaining multi-scale pores as well as the effects of the prepared pores are summarized in the following subsections (Fig. 3).

##### 2.4.1. Pores formed by crossing of carbon fibers

In traditional carbon-fiber-based electrodes, the micron-scale pores formed by the intersection of carbon fibers are conducive to electrolyte's penetration [56]. The pore size distribution varies greatly. The results showed that the pore size of carbon felt is concentrated in the range of 40  $\mu\text{m}$  to 100  $\mu\text{m}$ . The peak pore size distribution of carbon paper varies from 20  $\mu\text{m}$  to 60  $\mu\text{m}$  depending on the production process. In various carbon paper, the pore size distribution of SGL carbon paper is mostly similar to that of carbon felt and has the largest pore size. The carbon cloth shows obvious bimodal characteristics: Specifically, large pores of tens of microns are formed between the fiber bundles, and pores of only a few microns were formed between the fibers [11]. Ma et al. simulated the electrochemical performance of electrodes under different pore sizes and obtained the optimal pore size distribution under different porosity by a two-dimensional model [49]. Carbon paper electrodes are widely used to reduce ohmic polarization. Since carbon paper is mainly prepared by short fiber bonding, the internal pore size distribution is small, which is not conducive to electrolyte flow. And due to the introduction of the flow field, the mass transfer in the electrode mainly relies on diffusion and convection under the ribs, and the mass transfer ability of the carbon paper is further weakened. Mayrhuber created micron-scale pores in carbon paper using laser perforation. Although a part of the specific surface area of the carbon paper was lost in this way, by increasing the electrolyte convection channel, the permeability was improved, and the accessible specific surface area of the electrode was increased instead [58]. To resolve the contradiction between the increased pore size and reduced specific surface area, the crossing of the carbon fibers can be alerted through the design of fiber structure or the use of additives. For example, the ECSA of SGL carbon paper is more than five times larger than that of carbon felt with the similar pore size distribution. This enhancement can be attributed to the binders in carbon paper. By controlling the concentration of the precursors during the electrospinning process, Sun et al. assembled multiple carbon fibers into fiber bundles which formed large pores while hollow channels were constructed in the fibers to maintain relatively large specific surface area. Compared to the electrodes prepared through the traditional electrospinning method, the energy efficiency of the electrodes with the new structure was increased by 15.2 % [59].

Carbon fiber electrodes prepared by conventional electrospinning

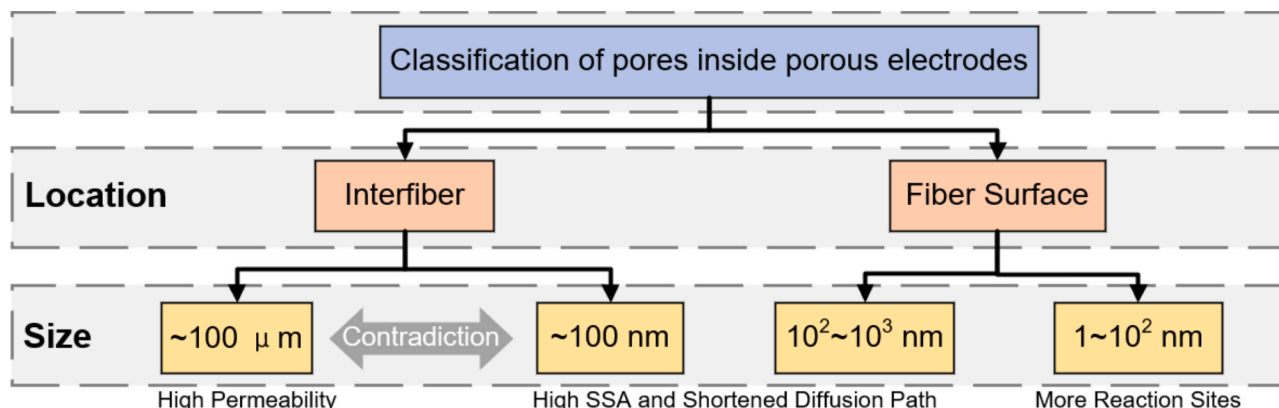


Fig. 3. Classification of pores inside porous electrodes.

have similar problems. This kind of electrode has low porosity and poor permeability, which causes great resistance to mass transfer. Xu et al. designed and fabricated a carbon nanofiber web with super-large pores by means of horizontal counter-blending electrospinning. The electrochemical impedance spectroscopy (EIS) results showed that the concentration polarization of the battery was effectively reduced due to the large pore size, and the electrolyte utilization rate was twice that of the conventional electrospun electrode [60].

#### 2.4.2. Pores on surface of carbon fiber

While a number of researchers optimized the pore-scale structure of the carbon fiber electrode, some researchers also tried to etch the carbon fiber surface to derive new pores [61,62].

The mesopores on the carbon fiber surface can increase the specific surface area of the electrode [52,63,64]. It can also shorten the ion diffusion distance to enhance the diffusion capacity. Wang reconstructed the electrode pore-scale structure by X-ray tomography. The simulation results showed that the addition of mesopores could interfere with the flow of the electrolyte, thereby increasing the degree of turbulence and the local flow velocity of the electrolyte fluid. In addition to this, the number of mesopores also affects the permeability of the porous electrode. The simulation results showed that under the same flow rate, both the infiltration amount and the current density of the porous electrode increase with the increase of the number of mesopores. This may be due to changes in the contact characteristics of the electrode surface and water. Although the morphology of the mesopores also affects the electrochemical performance to a certain extent, its effect is far less than that caused by the number of mesopores [52].

In addition to increasing the specific surface area of electrodes, mesopores and micropores also effectively provide reaction sites for electrochemical reaction. The carbon atoms at the edge of the graphite microcrystalline layer on the carbon fiber have unpaired electrons due to the asymmetric force, yielding enhanced surface activity of carbon fibers. One of the most widely used etching approaches for enhancing surface activity is chemical treatment. Rajeev et al. etched nanoscale pores on the surface of carbon felt and increased the energy efficiency of the battery to 89 % by increasing the specific surface area and oxygen-containing functional groups [65]. The addition of nanocracks on the graphite felt surface provided an improved path for electrolyte flow and significantly improved electrolyte utilization [66]. Zhang et al. improved the electrochemical activity of graphite felt by etching on the graphite surface felt with KOH [67]. Zhou et al. used the CuO precipitation method to etch a nanoporous catalytic layer with a size of approximately 200 nm on graphite felt's surface [68]. Liu et al. compared pristine carbon felt, thermally-treated carbon felt, and superficially porous treated graphite felt. The results show that the superficially porous graphite felt has higher energy efficiency and discharge capacity due to the additional active sites [69]. Xu et al. designed an electrode with integrated micro- and nanostructures. A catalytic layer of oxygen-enriched gradient nanopores was formed on the electrode surface, which could effectively enhance the electrochemical reaction without affecting the mass transfer [70]. Previous studies focused primarily on the impacts of the distribution density of micro- and mesopores. However, there is still a lack of sufficient understanding on the mechanisms of pore structure parameters on reaction kinetics.

#### 2.5. Functional groups

Etching pores on carbon fibers also introduces functional groups on the surface of carbon fibers. For carbon fibers, it mainly refers to oxygen-containing functional groups and nitrogen-containing functional groups. It has been largely explored in previous studies that the introduction of oxygen-containing and nitrogen-containing functional groups through pretreatments on the fibers such as acid-base and thermal treatments effectively enhances the reaction kinetics of the electrode. Li et al. found

that the functional group C=O promoted the adsorption of positively charged ions [26,71,72], thereby catalyzing the conversion of the redox couples and reducing the activation polarization [73–75]. For example, in the flow battery with  $\text{VO}^{2+}$  and  $\text{VO}_2^+$  as the redox couple, the oxygen-containing functional groups promote the transfer of the oxygen atoms in the solution to approach  $\text{VO}^{2+}$  [76]. Another explanation is that the introduction of oxygen-containing functional groups increases the active site on the surface of the carbon fiber. Shao et al. believed that carbon atoms adjacent to oxygen and nitrogen had higher positive charge density to balance the negative charge of nitrogen and oxygen elements. These positively charged carbon atoms can serve as active sites. Hu et al. introduced a large number of oxygen-containing functional groups on the surface of carbon felt by chemical vapor deposition, which greatly improved the conductivity of the material of the material of the material, and the energy efficiency of the battery was increased by 7.1 % [77]. This technology has the potential to further promote the large-scale application of carbon-based electrodes, addressing their shortcomings in poor activity and enhancing their electrochemical performance for redox reactions. In a large battery with dimensions of 20 cm by 20 cm, it can maintain an energy efficiency of 86.4 % [78]. The main function of the nitrogen-containing functional group is to enhance the electronegativity of the material, thereby increasing the electronic conductivity. After the introduction of nitrogen atoms, the pentavalent electrons of nitrogen would bring additional charges so that the transfer of electrons from the electrode to the reactant became easier [79].

Another effect of oxygen-containing functional groups is to enhance the hydrophilicity of carbon fibers. Polyacrylonitrile-based carbon fiber electrodes typically have poor hydrophilicity [76], resulting in a low wetted area on the porous electrode surface and thus low reaction rate and electrolyte utilization. Most of the oxygen-containing functional groups are polar groups. The lone pair of electrons around the oxygen atom can form hydrogen bonds with water. Therefore, oxygen-containing functional groups are mostly hydrophilic groups, and the introduction of oxygen-containing functional groups can enhance the surface's wettability. Wang et al. confirmed the effect of oxygen-containing functional groups on the wettability of carbon fibers through the contact angle test. Nitrogen-containing groups also have similar properties of enhancing the hydrophilicity of carbon fibers [66]. The higher the content of oxygen-containing functional groups, the stronger the wettability of the electrode and the smaller the contact angle [62]. Except for electrospun fiber felts, most carbon-based electrodes (carbon cloth, graphite felt, and carbon paper) are hydrophobic to the electrolyte, probably due to the lack of functional groups and the high degree of graphitization that leads to the lack of polar sites on their surface and the inability to attract water molecules [81]. Therefore, compared with other tested electrodes, the electrospun fiber mat is more favorable for the penetration of the electrolyte. This facilitates the efficient utilization of active sites on the fiber surface.

Although many studies have shown that oxygen-containing functional groups may improve the electrochemical activity of electrodes, some studies have suggested that this may have a negative effect on the redox process [82–85]. First, the electron transfer resistance will increase with the increase in the oxygen content, thereby increasing the ohmic overpotential [86]. Melke et al. found that the increase in oxygen-containing functional groups would reduce the  $\text{SP}^2\text{-C}$  content on the surface of carbon materials, affecting the charge transfer process [87,88]. He believed that the reason for the improved electrochemical performance was more likely to be the introduction of surface defect sites. Blasi et al. investigated the optimal oxygen content for electrochemical performance enhancement. The results show that the electrocatalytic activity is greatly improved when the oxygen content is between 4 % and 5 %. When the oxygen content exceeds 5 %, the performance declines [89]. The surface characteristics such as specific surface area and micropores and oxygen-containing functional groups are usually changed at the same time during the surface treatment of electrode materials. Different researchers disagree on which of the two

has the more significant impact on reaction kinetics [90–94]. It has also become a vital issue to quantitatively distinguish the effects of these two factors and adjust their ratios to optimize electrode performance [82–85,95].

To summarize, the electrode surface is where the electrochemical reaction takes place. The active material gains and loses electrons at the reaction site on the electrode surface, and a redox reaction occurs. The larger the surface area of the electrode, the more sites are available for reactions. On the one hand, the pore structural properties of porous electrodes, such as porosity, fiber diameter, pore morphology, and pore size, will actively or passively affect the specific surface area of the electrode, thereby affecting the kinetics. On the other hand, the change in these parameters will also affect the flow paths within the porous electrode, resulting in the change in the permeability and mass transfer performance. In addition, when the porous electrode is installed in the battery, the pore-scale structure change caused by the compression will make it more difficult to predict and grasp the rules of the pore-scale structure design. At present, there are still few studies on this aspect. The difficulty in the structure optimization is that in the existing electrode structure, the specific surface area and permeability are in conflict with each other. Changing the pore-scale structure to improve the performance of one is bound to cost the other. The two need to be weighed in different systems to select the most appropriate structural parameters (Table 2).

### 3. Pore-scale structure design of electrode

In general, the main problem of carbon electrodes is the contradiction between specific surface area and permeability. Without changing the existing structure, adjusting the pore-scale parameters can easily lead to opposite effects on the surface area and permeability. At present, there are two main optimization ideas to breach the contradiction. One way is to construct a novel composite electrode composed of different pore structures. Another approach is to etch the fiber surface or add the additional catalytic layer to enhance the electrode reaction kinetics

**Table 2**  
Part of the key research on electrode microstructure parameters.

Authors	Year	Method or Technology	Key findings
Chen et al. [48]	2019	Simulation	The variable porosity electrode can enhance the uniformity of electrolyte flow and reduce the concentration polarization.
Niu et al. [15]	2017	Simulation	The increase in the length-diameter ratio of the cross-sectional shape would lead to a decrease in diffusivity.
Jervis et al. [54]	2018	XCT	When the compression ratio exceeded 50 %, every 5 % increase would increase the tortuosity by 6.2 % to 7.6 %.
Mayrhuber et al. [58]	2014	Laser perforation	Micron-scale pores can improve the permeability and accessible specific surface area.
Sun et al. [59]	2018	Electrospinning	Fiber bundles which formed large pores while hollow channels increased energy efficiency by 15.2 %.
Xu et al. [60]	2017	Electrospinning	Carbon nanofiber web with super-large pores doubled the electrolyte utilization rate.
Rajeev et al. [66]	2020	Electrode activation	The addition of nanocracks on the graphite felt surface provided an improved path for electrolyte flow and significantly improved electrolyte utilization.
Zhang et al. [67]	2016	KOH etching	KOH etched electrodes can achieve an energy efficiency of 64 % at 250 mA/cm <sup>2</sup> .

without affecting the main flow path.

#### 3.1. Combination optimization of interfiber pores

In the common carbon fiber electrodes, the woven electrodes can realize multi-scale pores. The results showed that the carbon cloth performed better than other forms of carbon electrode, such as felt and paper, thanks to the double-scale pores brought about by its woven structure [11]. With reference to this structure of carbon cloth, many researchers have designed electrode structures with different aperture combinations to improve battery performance [100–103]. One of the simplest ways to do this is to stack electrodes of different apertures on top of each other. Zhou et al. designed a double-layer thin film electrode, combining two carbon-based electrodes with different pore size [104]. These electrodes have higher energy efficiency than carbon electrodes with a single pore size.

In addition to preparing electrodes with different pore sizes, an alternative method is to connect electrodes with larger pores to a thin film catalytic layer. Although the thin film electrode has a high specific surface area and low resistance, its small pore size makes the permeability of this electrode low. Yao et al. also achieved high battery performance by spraying electrocatalyst tungsten trioxide/super activated carbon to the side of the electrode near the membrane (Fig. 4a,b) [105]. Inspired by this, Zhou et al. transferred the microporous catalytic layer to the surface of carbon fiber. Compared with traditional catalyst layers, the thickness was reduced from tens of microns to hundreds of nanometers (Fig. 4c–e). In this way, the length of the diffusion path of reaction ions could be greatly shortened, leading to the accelerated transport rate of reactants [68]. In addition to the combination of different pore sizes, the connection modes of pores with different sizes also need to be further explored.

#### 3.2. Gradient pores

Coupling pores of different sizes together is an optimal approach to make full use of the advantages of pores at different scales [56]. In addition to the combination of interfiber pores with different pore sizes as mentioned above, there is an alternative approach to combine the large interfiber pores with the mesopores on the fiber surface. The KOH activation treatment is a simple but effective way for treating carbon paper [106] and carbon cloth [107] to produce gradient pores. Zhou et al. drew on the dual-dispersed porous structure of heat pipe evaporator to activate carbon paper electrode with KOH (Fig. 5). The 5 nm diameter mesopores were formed on the surface of carbon fiber. These mesopores could be used as active sites for electrochemical reactions. Meanwhile, the specific surface area of the electrode was increased by 16 times. It interacted with the existing large pores (~10 μm) between the carbon fibers to improve the energy efficiency under a high current density. The pores were randomly connected from mesoporous pores at the nanometer scale to large pores at the scale of tens of microns [106]. The gradient-distributed NiCo<sub>2</sub>O<sub>4</sub> nanorod-composed graphite felt electrode prepared by Wang et al. achieves high electrical density, high energy efficiency, and long cycle life (Fig. 5b) [108].

The difference in the scale makes the ion transport in pores relatively slow [109,110]. Reasonable design of pore structure requires optimization on multiple spatial scales. It is a new coupling method that researchers were trying to generate smaller pores in large and orderly mesopores. Wang et al. used chemical solution etching to generate three different scale gradient pore structures inside the graphite felt electrode (Fig. 5c–e). The carbon fibers crossed to form micron pores, which provide a flow path for electrolyte flow. Pores with diameters of 500 nm and 20 nm were distributed on the surface of the carbon fiber. The key to such gradient pore structure rested in the pores with diameters close to 500 nm they provide sufficient area to accommodate pores with diameters of 20 nm and shorten the diffusion distance of active substances for reaching the active site on the electrode surface for redox reaction.

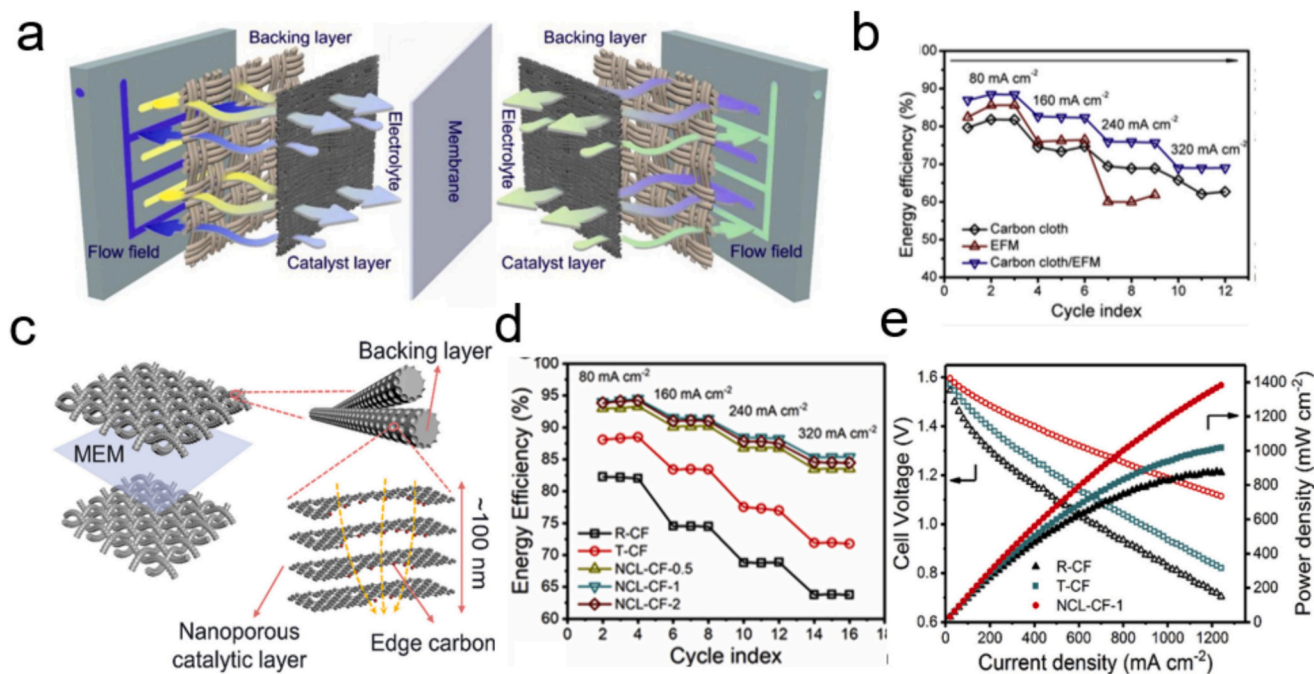


Fig. 4. (a) Schematic of the dual-layer electrode structured flow cell and (b) voltage efficiency. Adapted with permission from Ref. [105]. (c) Schematic of nanoporous catalytic layer structured carbon felt electrode architecture. (d) energy efficiency. and (e) polarization curves of batteries assembled with different electrodes. Adapted with permission from Ref. [68].

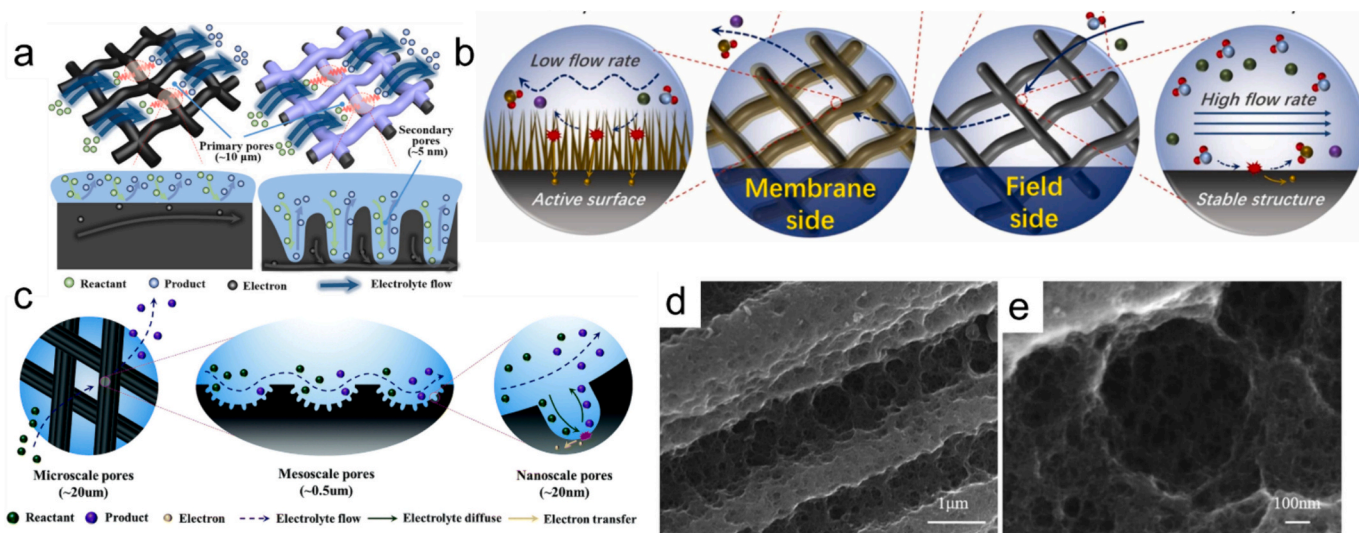


Fig. 5. (a) Schematic of the conventional carbon-fiber based electrode and the proposed dual-scale porous carbon electrode. (b) Schematic of the gradient-distributed NiCo<sub>2</sub>O<sub>4</sub> nanorod-composed graphite felt electrode [108]. (c) Schematic of the gradient-pore graphite felt electrodes. (d) (e) SEM image of gradient-pore graphite felt. Adapted with permission from Ref. [62].

The electrode showed high energy efficiency, high current density, and large discharge capacity in the battery cycle test [62].

### 3.3. Arrangement of carbon fibers

Conventional carbon-fiber electrodes are arranged in a disordered, random manner. The electrolyte flows through the pores between the carbon fibers. Such a flow path has a high tortuosity and high flow resistance. Limited by current manufacturing technology, most of the optimization of fiber arrangement is achieved by electrospinning. Flox et al. prepared carbon nanofibers with different order degrees by electrospinning (Fig. 6a). They concluded that the nanofibers with higher

order had higher electrical conductivity and were more conducive to electron transfer [111]. Zhao's team made carbon fiber electrodes aligned directionally also by electrospinning (Fig. 6c-e). The parallel arrangement of the carbon fibers made the electrodes loose in the plane. The electrolyte penetrated more easily in the plane. The limiting current density was 75 % higher than that of conventional electrospinning felt batteries [18].

The electrolyte penetrates into the electrode along the parallel and perpendicular direction of the electrode. The existing literature mainly focuses on the permeability perpendicular to the electrode direction. There is a lack of research and optimization on the permeability in the in-plane direction. For the electrode structure with flow field, the

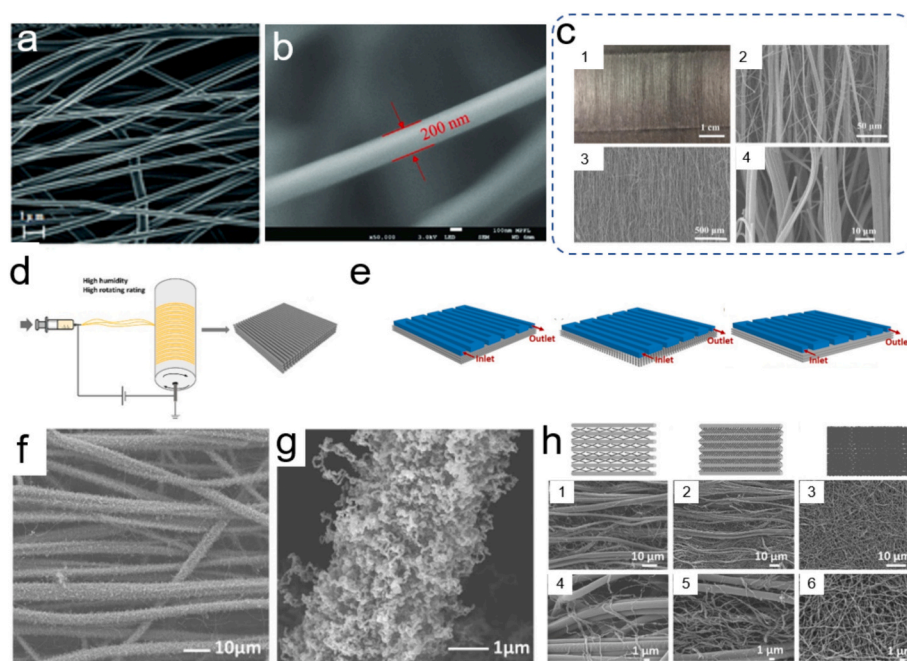


**Fig. 6.** (a) SEM images of prepared electrodes. Adapted with permission from Ref. [111]. (b) SEM images of aligned carbon nanofiber electrodes. Adapted with permission from Ref. [17]. (c) Digital photo of the aligned electrospun mat and SEM images of the aligned ECFs under different magnifications. Adapted with permission from Ref. [18]. (d) (e): 3D view of the serpentine channels with different orientations of aligned fiber electrodes. Adapted with permission from Ref. [18]. (f) (g): SEM images of the CNF-AECF electrodes. Adapted with permission from Ref. [112]. (h) Schematic illustration, SEM images at low magnification and high-resolution SEM images. Adapted with permission from Ref. [113].

distribution of under-the rib active species should be paid particular attention. Zhao et al. arranged electrospun carbon fiber electrodes in different directions in a flow cell. The results showed that the electrode direction was perpendicular to the direction of the flow channel yielding the best mass transfer ability [18].

Zhao's team did the same with electrospun carbon nanofibers (Fig. 6b). Carbon nanofibers have a smaller diameter and a higher specific surface area than conventional electrospun carbon fibers. However, the traditional electrospinning carbon nanofibers have the disadvantages of low porosity and poor hydrophilicity. The distribution and penetration of electrolyte could be improved by the directional arrangement of carbon nanofibers, and the concentration polarization can thus be greatly reduced. The aligned carbon nanofiber electrodes yielded higher limiting current density and higher charge-discharge capacity [17].

In addition, they have made other modifications to the oriented electrospinning fiber. They designed an aligned fiber electrode consisting of curved nanofibers growing on the surface (Fig. 6f,g) [112] and a composite electrode composed of aligned nanofibers as a skeleton and high porosity nanofibers as a filler (Fig. 5h) [113].

In conclusion, the optimization of electrode structures in flow batteries plays a crucial role in enhancing their performance and addressing challenges such as low power density and energy storage capacity. By designing and engineering the electrode materials, morphology, and architecture, researchers aim to improve the charge transfer kinetics, electrolyte accessibility, and overall electrochemical reactions within the battery system. However, the electrode structure optimization in the laboratory still has a long way from practical application, and both the preparation difficulty and the cost need to be further reduced.

#### 4. Manufacturing process of electrode

3D printing was invented in the 1980s. In recent years, 3D printing technology has been gradually used to prepare porous electrode structures in labs [19,20,21,33,34,114–121]. Compared with conventional

technologies, the 3D printing technology has unique advantages. One is that additive manufacturing saves more raw materials than subtractive manufacturing. The second is that specific internal structures can be realized in the process of building products through the layer-by-layer deposition of materials. The third is that small quantities of production can be achieved and cost savings [119]. It is expected to realize the optimized pore-scale structure precisely in the future, to tailor the electrode's characteristics to maximize its performance.

Selective laser melting technology and fused deposition manufacturing of 3D printing technology has been used to make the electrode material. Fused deposition manufacturing is often used in polymer processing and manufacturing. The most serious technical difficulty is the selection and preparation of ink. In order to achieve the ideal rheological properties of 3D printing, inks with high viscosity and absolute dilution properties are necessary. Graphene oxide has unique viscoelasticity in the aqueous solution, without adding polymer to control the concentration. Lacey et al. synthesized a water-based 3D printing ink through porous graphene oxide [117]. This ink was used to prepare an electrode structure with three levels of pores. It consisted of pores of 4 to 25  $\mu\text{m}$  in the porous graphene itself, pores of several tens of microns in the printed grid, and large pores of  $<500 \mu\text{m}$  formed on the printed filament. Such a multi-modal electrode could significantly increase the specific surface area and the number of active sites, which was beneficial to energy storage devices such as redox flow batteries that utilize interface reactions. However, 3D printing is not perfect. Most 3D printing techniques can only create one or two parts of a device, but not an entire portion. In addition, the majority of 3D printing technologies now available are unable to directly achieve the creation of intricate constructions with hierarchical porous structures at the micro-or nano-scale. Despite the tremendous advancements made in recent years, several obstacles still need to be overcome before 3D printing may be used directly as a manufacturing technique for the mass production of electrochemical energy storage devices. One of the major obstacles to fabricating electrochemical energy storage devices using 3D printing is the lack of materials that can be tailored to this new technology. For

mass production, it is necessary to get effective 3D printing to boost production rates and guarantee product quality and consistency while maintaining low manufacturing costs [122].

Electrospinning technology applies electrostatic force to the solution or molten polymer between two electrodes to prepare sub-micron to nano-scale fibers. Although the pore structure prepared by electrospinning is not completely controllable, the pore structure can be controlled to a certain extent by adjusting the solution parameters, process parameters, and environmental parameters [123]. Suzuki et al. also performed a single-parameter optimization of the carbon fiber diameter. The results showed that the electrode polarization loss was minimal when the fiber diameter was 4  $\mu\text{m}$  [124]. At present, most carbon fiber electrodes on the market have a diameter of about 5 to 10  $\mu\text{m}$ , which is large in diameter and limited in choice [56]. The fiber diameter has different optimal choices for different electrode materials. The research results show that using a larger fiber diameter for a battery system with good kinetic performance is beneficial for the active material to reach the electrode surface. Electrodes with poor kinetic properties are suitable for using smaller fiber diameters to ensure the reaction rate [125,126]. Using electrospinning is a way to obtain carbon fiber electrodes with a broader range of diameters. The carbon fiber diameter can be linearly regulated by adjusting the relevant parameters of the electrospinning process [124].

The researchers have achieved flexible control of pore structure parameters through electrospinning technology. Such as a double-diameter carbon fiber electrode [113]. The energy efficiency of the battery using double-diameter electrodes could reach 79.3 % at a current density of 400  $\text{mA}/\text{cm}^2$ . In addition to improving the pore-scale parameters of porous fiber electrodes, many novel porous fibers with pore structures such as spider web [127], dendritic [128], porous networks [129], core-shell [130], hollow [131], ribbon [132], etc., have also been prepared. Although these novel structures have not been fully applied to the field of electrochemistry, they provide guidance for the design of electrode microstructures.

Electrospun nanofiber-based electrodes exhibit remarkable rate capability and cycling stability, while the slow yielding rate of electrospun nanofibers significantly hinders large-scale production in industrial applications. At present, some novel electrospun devices can offer higher efficiency, while a further decrease in production cost and improvement in nanofiber qualities are necessary for practical considerations of them in the future. As for the long term, it is anticipated to

produce uniform fibers with high reproducibility at a mass-production level while ensuring the desired size, morphology, structure, and other properties [133].

## 5. Measurement for porous electrodes

With the development of electrode preparation technology, electrode preparation has reached the micro-nano scale. However, the mechanism of electrode's microstructure has been studied and speculated to some extent. It still needs to be measured and verified through experiments.

The most widely used method for characterizing battery-scale current distribution is to use a segmented battery setup. Hsieh measured the local current of the two batteries whose collector plate and the graphite plate were divided, respectively (Fig. 7a) [134]. The researchers divided the collector plate or graphite plate of the two cells into 25 segments and measured the current density of each segment. The results showed that the second scheme, i.e., segmented graphite plates, can eliminate the influence of in-plane lateral current on the local current density. However, this method will increase the contact resistance of the battery, causing the battery performance to drop significantly. In order to reduce the contact resistance, Clement et al. improved the segmented battery setup by using a printed circuit board [22]. Nevertheless, the resolution scale of the segmented battery was large, which cannot meet the demand for refined measurement.

In addition to the segmented battery setup, the researchers also tried to install probes inside the battery to measure the distribution of the local current or potential directly. Liu et al. arranged a potential probe in the center of each layer of carbon paper [136]. The probe was made of platinum, with a layer of polytetrafluoroethylene attached to the surface for insulation. The platinum probe tip was exposed to the electrolyte. This method could measure the vertical distribution of local electric potential in the multilayer carbon paper electrode. According to the local overpotential, the position of the active material in the electrode could be further determined. By the difference in the arrangement of the probes, the potential distribution in the electrode plane could also be measured. Becker et al. arranged carbon fiber point probes on the surface of the graphite felt and measured the potential distribution at different positions on the surface of the carbon felt (Fig. 7c) [137]. The polarization curve was measured by the potentiostatic method. And the current density distribution was deduced from the polarization curve.

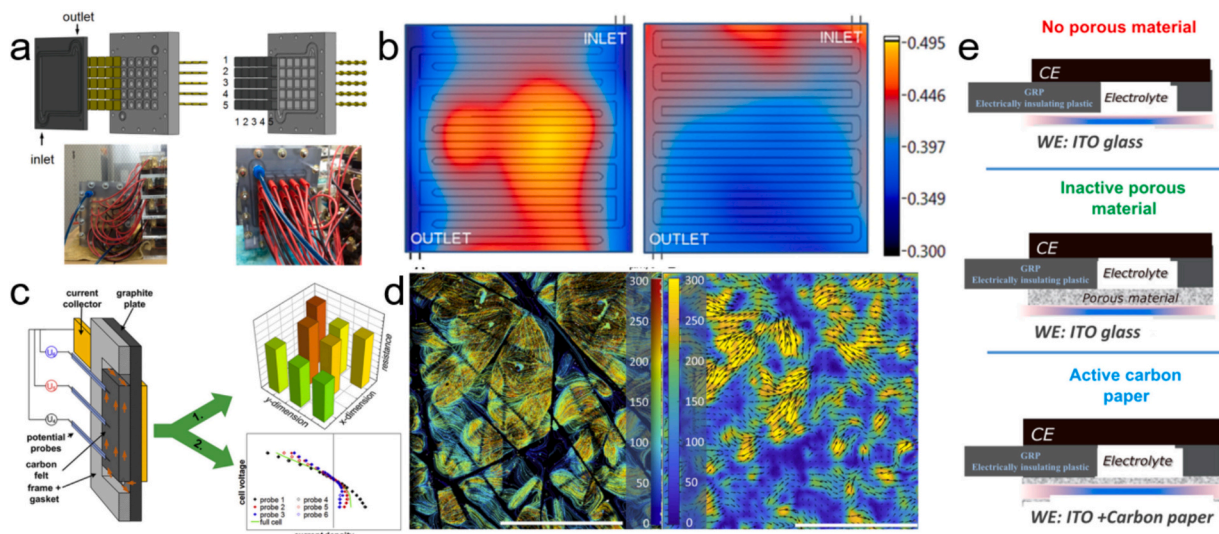


**Fig. 7.** (a) Schematics and photos of the two cell designs. Adapted with permission from Ref. [134]. (b) Experimentally measured current distribution. Adapted with permission from Ref. [138]. (c) Carbon fiber point probes on the surface of the graphite felt. Adapted with permission from Ref. [137]. (d) Fluorescent particle flow imaging within a porous carbon electrode. Adapted with permission from Ref. [139]. (e) Description of different ECL reactor operation modes. Adapted with permission from Ref. [140].

Chen et al. installed potential probes in half cells. In this way, the polarization loss of redox flow battery and the reaction distribution in the electrode was measured and researched.

In addition to the current and potential, the measurement of the distribution of active materials in the electrolyte is also an important research direction. But this field has not been studied too much. Only a few research teams conducted a qualitative analysis of the concentration distribution. Houser used a thermally responsive layer to visualize the electrolyte distribution (Fig. 7b) [138]. The thermosensitive liquid crystal film was placed between the positive and negative electrodes to replace the ion exchange membrane. They directly observed the color change of the thermal liquid crystal film through the processing window on the end plate. The convective flow and heat transfer of the electrolyte would cause the color change response of the corresponding area of the liquid crystal panel. In this way, the electrolyte flow could be directly visualized. The local current distribution obtained by other methods and the electrolyte flow could also be connected for qualitative analysis. Javier et al. used electrochemiluminescence imaging technology to detect the mass transfer phenomenon of the active material in the electrode of the redox flow battery (Fig. 8) [140]. The results showed that the electrolyte distribution in the electrode was not uniform, and the concentration of the electrolyte varies greatly in different regions. Wong et al. directly observed and qualitatively analyzed the reaction and mass transfer processes within porous electrodes using fluorescence microscopy (Fig. 7d,e) [139,141]. Observation accuracy could be accurate to tens of microns. The results showed that the electrolyte distribution and reaction were not uniform at this scale. The nonuniformity had a great influence on the performance of the battery. The flow characteristics of carbon paper electrodes from the same supplier were also different at the pore scale. This indicated that in addition to the microscopic characteristics such as porosity, permeability, and specific surface area, other structural characteristics in the porous electrode also greatly influence the transfer and reaction of active materials.

Using the above methods, only the macroscopic distribution of the electrolyte inside the electrode can be observed. To obtain pore-scale flow features, higher-precision detection techniques are required. Pore-scale features of porous electrodes can be acquired using computed tomography techniques. It can be used to characterize multiphase flow problems in porous media. Farid et al. used time-resolved 3D X-ray

tomography to image electrodes and the electrolyte in situ [142]. They processed and recognized grayscale images. The pore-scale flow and wetting phenomena were investigated. The permeation rule of electrolyte in porous electrode was explored. Kerstin et al. used X-ray computed tomography(CT) technology to visualize the process of electrolyte infiltration into carbon felt and studied the filling of electrolyte [143]. It provided a reference for improving the accessible specific surface area of electrodes. To further understand the characteristics of electrode concentration and current distribution on the pore-scale, an effective method is to reconstruct the three-dimensional structure of porous electrodes by CT and simulate the electrode microstructure by LBM. Zhang et al. used this method to simulate three kinds of carbon-based electrodes [144]. The results showed that the simulation results of this method were in good agreement with the experimental results, and the electrochemical performance of electrodes with different pore size distributions was significantly different.

## 6. Conclusions

The microscopic properties of carbon-based electrodes in flow batteries have a large impact on electrode performance and battery performance. Understanding its mechanism plays a vital role in designing and preparing electrode microstructures. The improvement of electrode performance is inseparable from the optimization and design of the electrode microstructure. The current research focusing on the mechanism of electrode microstructure, optimized design, preparation, and characterization are as follows:

- (1) Porosity and the electrode surface area are the most important basic microscopic properties. The two conflict with each other. A high-performance electrode should consider these two characteristics and strike a balance between low concentration polarization and high reaction kinetics.
- (2) At present, researchers' main optimization methods include gradient pore structure, catalytic layer on the electrode surface, and aligned carbon fiber. Despite the significant enhancements in electrode performance achieved by these optimized electrodes, the path forward is not without challenges. One of the main hurdles is the scalability of these advanced microstructures.

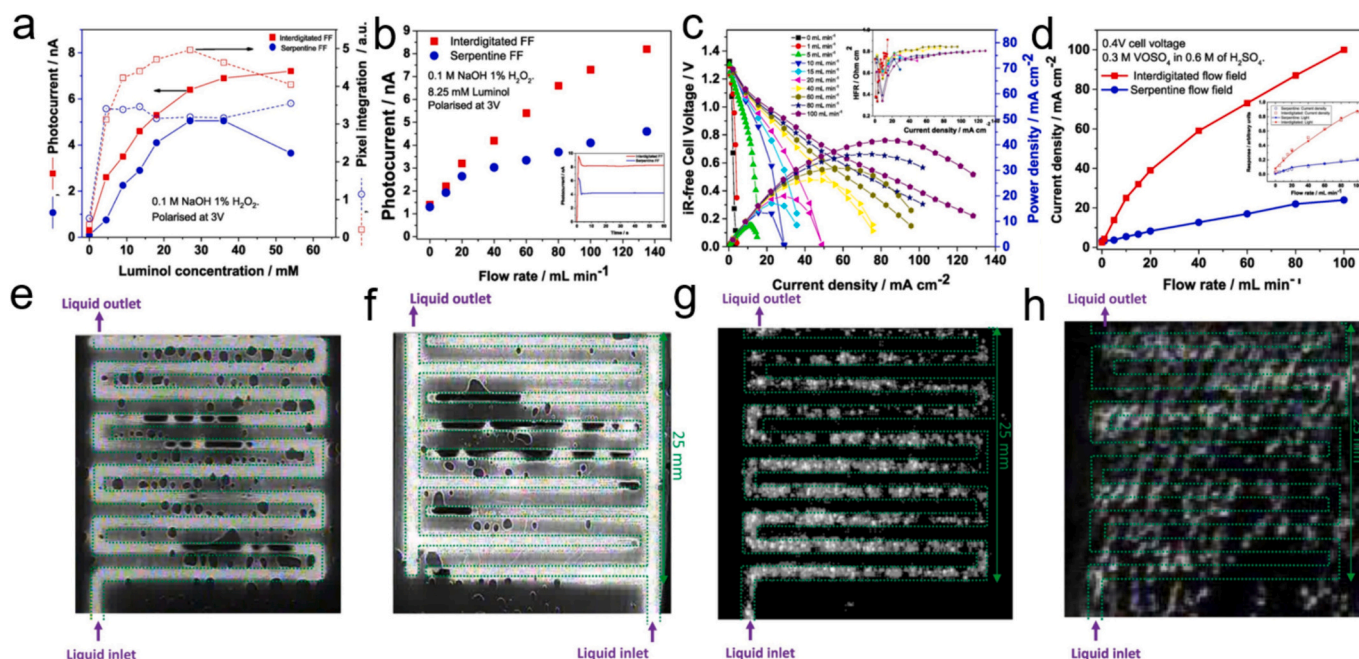


Fig. 8. (a)–(d): Luminol ECL compared to RFB performance. (e)–(h): Mass transport visualization showing the effect of FF. Adapted with permission from Ref. [140].

While nanostructured materials can provide excellent performance at the laboratory scale, translating this to industrial production while maintaining cost-effectiveness is a complex task. Additionally, the durability of these intricate structures under the rigorous conditions of flow battery operation is a critical concern that requires further investigation. Another challenge is the balance between performance and complexity. As we aim to refine the microstructure, we must also consider the practicality of the design, ensuring that the manufacturing process does not become overly complicated or expensive. The development of robust, yet manufacturable, electrode designs is a key area that demands attention.

- (3) Current electrode materials have been enhanced through novel manufacturing techniques such as 3D printing and electrostatic spinning, which offer distinct advantages for micro-scale electrode processing and have been shown to significantly improve performance. However, research on the direct design and processing of microstructures remains scarce. Additionally, current qualitative analysis methods are limited, with measurement accuracies typically at the millimeter scale, and no advanced characterization or visualization techniques are available for the micro-scale.

#### CRediT authorship contribution statement

**Pengfei Wang:** Writing – original draft, Investigation, Formal analysis. **Yijian Zhao:** Writing – original draft, Investigation, Formal analysis. **Yuhang Ban:** Investigation, Formal analysis. **Menglian Zheng:** Writing – review & editing, Supervision, Project administration, Funding acquisition.

#### Declaration of competing interest

The authors declare that they have no known competing financial interests or personal relationships that could have appeared to influence the work reported in this paper.

#### Data availability

No data was used for the research described in the article.

#### Acknowledgements

This work was supported by the Fundamental Research Funds for the Central Universities [grant number 2022ZFJH004], Hangzhou Science and Technology Commission [grant number 202204T13] and National Natural Science Foundation of China [grant number 51606164].

#### References

- [1] M. Skyllas-Kazacos, M.H. Chakrabarti, S.A. Hajimolana, F.S. Mjalli, M. Saleem, Progress in flow battery research and development, *J. Electrochem. Soc.* 158 (2011) R55, <https://doi.org/10.1149/1.3599565>.
- [2] K. Amini, A.N. Shocron, M.E. Suss, M.J. Aziz, Pathways to high-power-density redox flow batteries, *ACS Energy Lett.* 8 (2023) 3526–3535, <https://doi.org/10.1021/acsenerylett.3c01043>.
- [3] M.L. Perry, A.Z. Weber, Advanced redox-flow batteries: a perspective, *J. Electrochem. Soc.* 163 (2015) A5064, <https://doi.org/10.1149/2.0101601jes>.
- [4] M.L. Perry, K.E. Rodby, F.R. Brushett, Untapped potential: the need and opportunity for high-voltage aqueous redox flow batteries, *ACS Energy Lett.* 7 (2022) 659–667, <https://doi.org/10.1021/acsenerylett.1c02225>.
- [5] J. Winsberg, T. Hagemann, T. Janoschka, M.D. Hager, U.S. Schubert, Redox-flow batteries: from metals to organic redox-active materials, *Angew. Chem. Int. Edit.* 56 (2017) 686–711, <https://doi.org/10.1002/anie.201604925>.
- [6] R. Wang, Y. Li, H. Liu, Y.-L. He, M. Hao, Sandwich-like multi-scale hierarchical porous carbon with a highly hydroxylated surface for flow batteries, *J. Mater. Chem. A* 9 (2021) 2345–2356, <https://doi.org/10.1039/D0TA10284A>.
- [7] A. Abbas, S. Abbas, A. Bhattarai, N.M. Latiff, N. Wai, A.N. Phan, T.M. Lim, Effect of electrode porosity on the charge transfer in vanadium redox flow battery, *J. Power Sources* 488 (2021) 229411, <https://doi.org/10.1016/j.jpowsour.2020.229411>.
- [8] M.H. Chakrabarti, N.P. Brandon, S.A. Hajimolana, F. Tariq, V. Yufit, M. A. Hashim, M.A. Hussain, C.T.J. Low, P.V. Aravind, Application of carbon materials in redox flow batteries, *J. Power Sources* 253 (2014) 150–166, <https://doi.org/10.1016/j.jpowsour.2013.12.038>.
- [9] L. Eifert, Z. Jusys, R.J. Behm, R. Zeis, Side reactions and stability of pre-treated carbon felt electrodes for vanadium redox flow batteries: a DEMS study, *Carbon* 158 (2020) 580–587, <https://doi.org/10.1016/j.carbon.2019.11.029>.
- [10] Z. Hu, Z. Miao, Z. Xu, X. Zhu, F. Zhong, M. Ding, J. Wang, X. Xie, C. Jia, J. Liu, Carbon felt electrode modified by lotus seed shells for high-performance vanadium redox flow battery, *Chem. Eng. J.* 450 (2022) 138377, <https://doi.org/10.1016/j.cej.2022.138377>.
- [11] A. Forner-Cuenca, E.E. Penn, A.M. Oliveira, F.R. Brushett, Exploring the role of electrode microstructure on the performance of non-aqueous redox flow batteries, *J. Electrochem. Soc.* 166 (2019) A2230–A2241, <https://doi.org/10.1149/2.0611910jes>.
- [12] B.A. Simon, A. Gayon-Lombardo, C.A. Pino-Muñoz, C.E. Wood, K.M. Tenny, K. V. Greco, S.J. Cooper, A. Forner-Cuenca, F.R. Brushett, A.R. Kucernak, N. P. Brandon, Combining electrochemical and imaging analyses to understand the effect of electrode microstructure and electrolyte properties on redox flow batteries, *Appl. Energy* 306 (2022) 117678, <https://doi.org/10.1016/j.apenergy.2021.117678>.
- [13] J. Kim, H. Park, Recent advances in porous electrodes for vanadium redox flow batteries in grid-scale energy storage systems: a mass transfer perspective, *J. Power Sources* 545 (2022) 231904, <https://doi.org/10.1016/j.jpowsour.2022.231904>.
- [14] D. Emmel, J.D. Hofmann, T. Arlt, I. Manke, G.D. Wehinger, D. Schröder, Understanding the impact of compression on the active area of carbon felt electrodes for redox flow batteries, *ACS Appl. Energy Mater.* 3 (2020) 4384–4393, <https://doi.org/10.1021/acsaem.0c00075>.
- [15] Y. Niu, W. Lv, G. Rao, W. He, J. He, A critical look into effects of electrode pore morphology in solid oxide fuel cells, *AICHE J.* 63 (2017) 2312–2317, <https://doi.org/10.1002/aic.15554>.
- [16] V. Muñoz-Perales, P.A. García-Salaberrí, A. Mularczyk, S. Enrique Ibáñez, M. Vera, A. Forner-Cuenca, Investigating the coupled influence of flow fields and porous electrodes on redox flow battery performance, *J. Power Sources* 586 (2023) 233420, <https://doi.org/10.1016/j.jpowsour.2023.233420>.
- [17] Z. Zhang, B. Bai, L. Zeng, L. Wei, T. Zhao, Aligned electrospun carbon nanofibers as electrodes for vanadium redox flow batteries, *Energy Technol.* 7 (2019) 1900488, <https://doi.org/10.1002/ente.201900488>.
- [18] J. Sun, H.R. Jiang, B.W. Zhang, C.Y.H. Chao, T.S. Zhao, Towards uniform distributions of reactants via the aligned electrode design for vanadium redox flow batteries, *Appl. Energy* 259 (2020) 114198, <https://doi.org/10.1016/j.apenergy.2019.114198>.
- [19] C.-Y. Lee, A.C. Taylor, A. Nattestad, S. Beirne, G.G. Wallace, 3D printing for electrocatalytic applications, *Joule* 3 (2019) 1835–1849, <https://doi.org/10.1016/j.joule.2019.06.010>.
- [20] J. Lölsberg, O. Starck, S. Stiefel, J. Hereijgers, T. Breugelmans, M. Wessling, 3D-printed electrodes with improved mass transport properties, *ChemElectroChem* 4 (2017) 3309–3313, <https://doi.org/10.1002/celec.201700662>.
- [21] G. Luo, K.S. Teh, Y. Liu, X. Zang, Z. Wen, L. Lin, Direct-write, self-aligned electrospinning on paper for controllable fabrication of three-dimensional structures, *ACS Appl. Mater. Interfaces* 7 (2015) 27765–27770, <https://doi.org/10.1021/acsaami.5b08909>.
- [22] J.T. Clement, T.A. Zawodzinski, M.M. Mench, Measurement of localized current distribution in a vanadium redox flow battery, *ECS Trans.* 58 (2014) 9–16, <https://doi.org/10.1149/05837.0009ecst>.
- [23] D. Maggiolo, F. Zanini, F. Picano, A. Trovò, S. Carmignato, M. Guarnieri, Particle based method and X-ray computed tomography for pore-scale flow characterization in VRFB electrodes, *Energy Storage Mater.* 16 (2019) 91–96, <https://doi.org/10.1016/j.ensm.2018.04.021>.
- [24] D. Aaron, Z. Tang, A.B. Papandrew, T.A. Zawodzinski, Polarization curve analysis of all-vanadium redox flow batteries, *J. Appl. Electrochem.* 41 (2011) 1175–1182, <https://doi.org/10.1007/s10800-011-0335-7>.
- [25] R. Wang, Bi-layer graphite felt as the positive electrode for zinc-bromine flow batteries: achieving efficient redox reaction and stable mass transport, *J. Energy Storage* 74 (2023) 109487, <https://doi.org/10.1016/j.est.2023.109487>.
- [26] F. Qiu, D. Harrison, J. Fyson, D. Southee, Fabrication and characterisation of flexible coaxial thin thread supercapacitors, *Smart Sci.* 2 (2014) 107–115, <https://doi.org/10.1080/23080477.2014.11665613>.
- [27] N. Böckenfeld, S.S. Jeong, M. Winter, S. Passerini, A. Balducci, Natural, cheap and environmentally friendly binder for supercapacitors, *J. Power Sources* 221 (2013) 14–20, <https://doi.org/10.1016/j.jpowsour.2012.07.076>.
- [28] B. Philip, E. Jewell, P. Greenwood, C. Weirman, Material and process optimization screen printing carbon graphite pastes for mass production of heating elements, *J. Manuf. Process.* 22 (2016) 185–191, <https://doi.org/10.1016/j.jmapro.2016.03.001>.
- [29] K. Yang, R. Torah, Y. Wei, S. Beeby, J. Tudor, Waterproof and durable screen printed silver conductive tracks on textiles, *Text. Res. J.* 83 (2013) 2023–2031, <https://doi.org/10.1177/0040517513490063>.
- [30] H.T. Jeong, B.C. Kim, M.J. Higgins, G.G. Wallace, Highly stretchable reduced graphene oxide (rGO)/single-walled carbon nanotubes (SWNTs) electrodes for energy storage devices, *Electrochim. Acta* 163 (2015) 149–160, <https://doi.org/10.1016/j.electacta.2015.02.022>.
- [31] J. Yeo, G. Kim, S. Hong, M.S. Kim, D. Kim, J. Lee, H.B. Lee, J. Kwon, Y.D. Suh, H. W. Kang, H.J. Sung, J.-H. Choi, W.-H. Hong, J.M. Ko, S.-H. Lee, S.-H. Choa, S. H. Ko, Flexible supercapacitor fabrication by room temperature rapid laser

- processing of roll-to-roll printed metal nanoparticle ink for wearable electronics application, *J. Power Sources* 246 (2014) 562–568, <https://doi.org/10.1016/j.jpowsour.2013.08.012>.
- [33] L.F. Arenas, C. Ponce de León, F.C. Walsh, 3D-printed porous electrodes for advanced electrochemical flow reactors: a Ni/stainless steel electrode and its mass transport characteristics, *Electrochem. Commun.* 77 (2017) 133–137, <https://doi.org/10.1016/j.elechem.2017.03.009>.
- [34] M. Areir, Y. Xu, R. Zhang, D. Harrison, J. Fyson, E. Pei, A study of 3D printed active carbon electrode for the manufacture of electric double-layer capacitors, *J. Manuf. Process.* 25 (2017) 351–356, <https://doi.org/10.1016/j.jmapro.2016.12.020>.
- [35] C. Kim, K.S. Yang, Electrochemical properties of carbon nanofiber web as an electrode for supercapacitor prepared by electrospinning, *Appl. Phys. Lett.* 83 (2003) 1216–1218, <https://doi.org/10.1063/1.1599963>.
- [36] S. Kaushal, P. Negi, A.K. Sahu, S.R. Dhakate, Upshot of natural graphite inclusion on the performance of porous conducting carbon fiber paper in a polymer electrolyte membrane fuel cell, *J. Mater. Res. Express* 4 (2017) 095603, <https://doi.org/10.1088/2053-1591/aa8517>.
- [37] R. Taherian, M. Matboo Ghorbani, S.R. Kiahosseini, A new method for optimal fabrication of carbon composite paper as gas diffusion layer used in proton exchange membrane of fuel cells, *J. Electroanal. Chem.* 815 (2018) 90–97, <https://doi.org/10.1016/j.jelechem.2018.03.009>.
- [38] C. Lei, F. Markoulidis, P. Wilson, C. Lekakou, Phenolic carbon cloth-based electric double-layer capacitors with conductive interlayers and graphene coating, *J. Appl. Electrochem.* 46 (2016) 251–258, <https://doi.org/10.1007/s10800-015-0909-x>.
- [39] S.R. Tennison, Phenolic-resin-derived activated carbons, *Appl. Catal. A Gen.* 173 (1998) 289–311, [https://doi.org/10.1016/S0926-860X\(98\)00186-0](https://doi.org/10.1016/S0926-860X(98)00186-0).
- [40] X. Ke, J.M. Prah, J.I.D. Alexander, J.S. Wainright, T.A. Zawodzinski, R. F. Savinell, Rechargeable redox flow batteries: flow fields, stacks and design considerations, *Chem. Soc. Rev.* 47 (2018) 8721–8743, <https://doi.org/10.1039/C8CS00072G>.
- [41] J.T. Gostick, M.W. Fowler, M.D. Pritzker, M.A. Ioannidis, L.M. Behra, In-plane and through-plane gas permeability of carbon fiber electrode backing layers, *J. Power Sources* 162 (2006) 228–238, <https://doi.org/10.1016/j.jpowsour.2006.06.096>.
- [42] J. Li, Y. Gu, Coalescence of oil-in-water emulsions in fibrous and granular beds, *Sep. Purif. Technol.* 42 (2005) 1–13, <https://doi.org/10.1016/j.seppur.2004.05.006>.
- [43] H.E. Pacella, H.J. Eash, B.J. Frankowski, W.J. Federspiel, Darcy permeability of hollow fiber bundles used in blood oxygenation devices, *J. Membr. Sci.* 382 (2011) 238–242, <https://doi.org/10.1016/j.memsci.2011.08.012>.
- [44] H.L. Liu, W.R. Hwang, Permeability prediction of fibrous porous media with complex 3D architectures, *Compos. A Appl. Sci. Manuf.* 43 (2012) 2030–2038, <https://doi.org/10.1016/j.compositesa.2012.07.024>.
- [45] R. Carta, S. Palmas, A.M. Polcaro, G. Tola, Behaviour of a carbon felt flow by electrodes part I: mass transfer characteristics, *J. Appl. Electrochem.* 21 (1991) 793–798, <https://doi.org/10.1007/BF01402816>.
- [46] A.Z. Weber, M.M. Mench, J.P. Meyers, P.N. Ross, J.T. Gostick, Q. Liu, Redox flow batteries: a review, *J. Appl. Electrochem.* 41 (2011) 1137–1164, <https://doi.org/10.1007/s10800-011-0348-2>.
- [47] W. Chen, J. Kang, Q. Shu, Y. Zhang, Analysis of storage capacity and energy conversion on the performance of gradient and double-layered porous electrode in all-vanadium redox flow batteries, *Energy* 180 (2019) 341–355, <https://doi.org/10.1016/j.energy.2019.05.037>.
- [48] C. Ma, X. Li, L. Lin, L. Chen, M. Wang, J. Zhou, A two-dimensional porous electrode model for designing pore structure in a quinone-based flow cell, *J. Energy Storage* 18 (2018) 16–25, <https://doi.org/10.1016/j.est.2018.04.007>.
- [49] L. Chen, A. He, J. Zhao, Q. Kang, Z.-Y. Li, J. Carmeliet, N. Shikazono, W.-Q. Tao, Pore-scale modeling of complex transport phenomena in porous media, *Prog. Energy Combust. Sci.* 88 (2022) 100968, <https://doi.org/10.1016/j.pecs.2021.100968>.
- [50] A. Duda, Z. Kozá, M. Matyka, Hydraulic tortuosity in arbitrary porous media flow, *Phys. Rev. E* 84 (2011) 036319, <https://doi.org/10.1103/PhysRevE.84.036319>.
- [51] M. Wang, J. Du, J. Zhou, C. Ma, L. Bao, X. Li, X. Li, Numerical evaluation of the effect of mesopore microstructure for carbon electrode in flow battery, *J. Power Sources* 424 (2019) 27–34, <https://doi.org/10.1016/j.jpowsour.2019.03.087>.
- [52] S. Song, Y. Liang, Z. Li, Y. Wang, R. Fu, D. Wu, P. Tsiakaras, Effect of pore morphology of mesoporous carbons on the electrocatalytic activity of Pt nanoparticles for fuel cell reactions, *Appl. Catal. B Environ.* 98 (2010) 132–137, <https://doi.org/10.1016/j.apcatb.2010.05.021>.
- [53] R. Jervis, M.D.R. Kok, T.P. Neville, C. Meyer, L.D. Brown, F. Iacoviello, J. T. Gostick, D.J.L. Brett, P.R. Shearing, In situ compression and X-ray computed tomography of flow battery electrodes, *J. Energy Chem.* 27 (2018) 1353–1361, <https://doi.org/10.1016/j.jechem.2018.03.022>.
- [54] J. Haber, Manual on catalyst characterization (Recommendations 1991), *Pure Appl. Chem.* 63 (1991) 1227–1246, <https://doi.org/10.1351/pac199163091227>.
- [55] Q. Wu, X. Zhang, Y. Lv, L. Lin, Y. Liu, X. Zhou, Bio-inspired multiscale-pore-network structured carbon felt with enhanced mass transfer and activity for vanadium redox flow batteries, *J. Mater. Chem. A* 6 (2018) 20347–20355, <https://doi.org/10.1039/C8TA06445H>.
- [56] I. Mayrhuber, C.R. Dennison, V. Kalra, E.C. Kumbur, Laser-perforated carbon paper electrodes for improved mass-transport in high power density vanadium redox flow batteries, *J. Power Sources* 260 (2014) 251–258, <https://doi.org/10.1016/j.jpowsour.2014.03.007>.
- [57] J. Sun, L. Zeng, H.R. Jiang, C.Y.H. Chao, T.S. Zhao, Formation of electrodes by self-assembling porous carbon fibers into bundles for vanadium redox flow batteries, *J. Power Sources* 405 (2018) 106–113, <https://doi.org/10.1016/j.jpowsour.2018.10.035>.
- [58] C. Xu, X. Li, T. Liu, H. Zhang, Design and synthesis of a free-standing carbon nano-fibrous web electrode with ultra large pores for high-performance vanadium flow batteries, *RSC Adv.* 7 (2017) 45932–45937, <https://doi.org/10.1039/C7RA07365H>.
- [59] C. Wang, X. Li, X. Xi, W. Zhou, Q. Lai, H. Zhang, Bimodal highly ordered mesostructure carbon with high activity for Br<sub>2</sub>/Br<sup>-</sup> redox couple in bromine based batteries, *Nano Energy* 21 (2016) 217–227, <https://doi.org/10.1016/j.nanoen.2016.01.015>.
- [60] R. Wang, Y. Li, Y.-L. He, Achieving gradient-pore-oriented graphite felt for vanadium redox flow batteries: meeting improved electrochemical activity and enhanced mass transport from nano- to micro-scale, *J. Mater. Chem. A* 7 (2019) 10962–10970, <https://doi.org/10.1039/C9TA00807A>.
- [61] Y. Lu, S. Zhang, J. Yin, C. Bai, J. Zhang, Y. Li, Y. Yang, Z. Ge, M. Zhang, L. Wei, M. Ma, Y. Ma, Y. Chen, Mesoporous activated carbon materials with ultrahigh mesopore volume and effective specific surface area for high performance supercapacitors, *Carbon* 124 (2017) 64–71, <https://doi.org/10.1016/j.carbon.2017.08.044>.
- [62] P. Wang, X. Zhang, H. Li, J. Hu, M. Zheng, Enhanced ion transport through mesopores engineered with additional adsorption of layered double hydroxides array in alkaline flow batteries, *Small* (2023) 2308791, <https://doi.org/10.1002/sml.202308791>.
- [63] R.K. Gautam, M. Kapoor, A. Verma, Tactical surface modification of a 3D graphite felt as an electrode of vanadium redox flow batteries with enhanced electrolyte utilization and fast reaction kinetics, *Energy Fuel* 34 (2020) 5060–5071, <https://doi.org/10.1021/acs.energyfuels.0c00701>.
- [64] R.K. Gautam, A. Verma, Uniquely designed surface nanocracks for highly efficient and ultra-stable graphite felt electrode for vanadium redox flow battery, *Mater. Chem. Phys.* 251 (2020) 123178, <https://doi.org/10.1016/j.matchemphys.2020.123178>.
- [65] Z. Zhang, J. Xi, H. Zhou, X. Qiu, KOH etched graphite felt with improved wettability and activity for vanadium flow batteries, *Electrochim. Acta* 218 (2016) 15–23, <https://doi.org/10.1016/j.electacta.2016.09.099>.
- [66] X. Zhou, X. Zhang, Y. Lv, L. Lin, Q. Wu, Nano-catalytic layer engraved carbon felt via copper oxide etching for vanadium redox flow batteries, *Carbon* 153 (2019) 674–681, <https://doi.org/10.1016/j.carbon.2019.07.072>.
- [67] Y. Liu, Y. Shen, L. Yu, L. Liu, F. Liang, X. Qiu, J. Xi, Holey-engineered electrodes for advanced vanadium flow batteries, *Nano Energy* 43 (2018) 55–62, <https://doi.org/10.1016/j.nanoen.2017.11.012>.
- [68] Z. Xu, W. Xiao, K. Zhang, D. Zhang, H. Wei, X. Zhang, Z. Zhang, N. Pu, J. Liu, C. Yan, An advanced integrated electrode with micron- and nano-scale structures for vanadium redox flow battery, *J. Power Sources* 450 (2020) 227686, <https://doi.org/10.1016/j.jpowsour.2019.227686>.
- [69] P. Chen, R.L. McCreery, Control of electron transfer kinetics at glassy carbon electrodes by specific surface modification, *Anal. Chem.* 68 (1996) 3958–3965, <https://doi.org/10.1021/ac960492r>.
- [70] W. Li, J. Liu, C. Yan, Reduced graphene oxide with tunable C/O ratio and its activity towards vanadium redox pairs for an all vanadium redox flow battery, *Carbon* 55 (2013) 313–320, <https://doi.org/10.1016/j.carbon.2012.12.069>.
- [71] G. Wei, Z. Gao, Z. Wei, X. Fan, J. Liu, C. Yan, Coupling effect between the structure and surface characteristics of electrospun carbon nanofibers on the electrochemical activity towards the VO<sub>2</sub><sup>+</sup>/VO<sup>2+</sup> redox couple, *Phys. Chem. Chem. Phys.* 17 (2015) 20368–20375, <https://doi.org/10.1039/C5CP02952J>.
- [72] M. Park, Y. Jung, J. Kim, H. Il Lee, J. Cho, Synergistic effect of carbon nanofiber/nanotube composite catalyst on carbon felt electrode for high-performance all-vanadium redox flow battery, *Nano Lett.* 13 (2013) 4833–4839, <https://doi.org/10.1021/nl402566s>.
- [73] W. Li, Z. Zhang, Y. Tang, H. Bian, T. Ng, W. Zhang, C. Lee, Graphene-nanowall-decorated carbon felt with excellent electrochemical activity toward VO<sub>2</sub><sup>+</sup>/VO<sup>2+</sup> couple for all vanadium redox flow battery, *Adv. Sci.* 3 (2016) 1500276, <https://doi.org/10.1002/adv.201500276>.
- [74] K.J. Kim, M.-S. Park, Y.-J. Kim, J.H. Kim, S.X. Dou, M. Skyllas-Kazacos, A technology review of electrodes and reaction mechanisms in vanadium redox flow batteries, *J. Mater. Chem. A* 3 (2015) 16913–16933, <https://doi.org/10.1039/C5TA02613J>.
- [75] H. Fu, X. Bao, M. He, J. Xu, Z. Miao, M. Ding, J. Liu, C. Jia, Defect-rich graphene skin modified carbon felt as a highly enhanced electrode for vanadium redox flow batteries, *J. Power Sources* 556 (2023) 232443, <https://doi.org/10.1016/j.jpowsour.2022.232443>.
- [76] T. Long, Y. Long, M. Ding, Z. Xu, J. Xu, Y. Zhang, M. Bai, Q. Sun, G. Chen, C. Jia, Large scale preparation of 20 cm × 20 cm graphene modified carbon felt for high performance vanadium redox flow battery, *Nano Res.* 14 (2021) 3538–3544, <https://doi.org/10.1007/s12274-021-3564-z>.
- [77] Y. Shao, X. Wang, M. Engelhard, C. Wang, S. Dai, J. Liu, Z. Yang, Y. Lin, Nitrogen-doped mesoporous carbon for energy storage in vanadium redox flow batteries, *J. Power Sources* 195 (2010) 4375–4379, <https://doi.org/10.1016/j.jpowsour.2010.01.015>.
- [78] S. Liu, M. Kok, Y. Kim, J.L. Barton, F.R. Brushett, J. Gostick, Evaluation of electrospun fibrous mats targeted for use as flow battery electrodes, *J. Electrochem. Soc.* 164 (2017) A2038–A2048, <https://doi.org/10.1149/2.1301709jes>.

- [82] M.V. Holland-Cunz, J. Friedl, U. Stimming, Anion effects on the redox kinetics of positive electrolyte of the all-vanadium redox flow battery, *J. Electroanal. Chem.* 819 (2018) 306–311, <https://doi.org/10.1016/j.jelechem.2017.10.061>.
- [83] J. Friedl, U. Stimming, Determining electron transfer kinetics at porous electrodes, *Electrochim. Acta* 227 (2017) 235–245, <https://doi.org/10.1016/j.electacta.2017.01.010>.
- [84] H. Fink, J. Friedl, U. Stimming, Composition of the electrode determines which half-cell's rate constant is higher in a vanadium flow battery, *J. Phys. Chem. C* 120 (2016) 15893–15901, <https://doi.org/10.1021/acs.jpcc.5b12098>.
- [85] S. Rümmler, M. Steimecke, S. Schimpf, M. Hartmann, S. Förster, M. Bron, Highly graphitic, mesoporous carbon materials as electrocatalysts for vanadium redox reactions in all-vanadium redox-flow batteries, *J. Electrochem. Soc.* 165 (2018) A2510, <https://doi.org/10.1149/2.1251810jes>.
- [86] D. Cheng, Y. Li, J. Zhang, M. Tian, B. Wang, Z. He, L. Dai, L. Wang, Recent advances in electrospun carbon fiber electrode for vanadium redox flow battery: properties, structures, and perspectives, *Carbon* 170 (2020) 527–542, <https://doi.org/10.1016/j.carbon.2020.08.058>.
- [87] S.M. Taylor, A. Pătru, D. Streich, M. El Kazzi, E. Fabbri, T.J. Schmidt, Vanadium (V) reduction reaction on modified glassy carbon electrodes – role of oxygen functionalities and microstructure, *Carbon* 109 (2016) 472–478, <https://doi.org/10.1016/j.carbon.2016.08.044>.
- [88] J. Melke, P. Jakes, J. Langner, L. Riekehr, U. Kunz, Z. Zhao-Karger, A. Nefedov, H. Sezen, C. Wöll, H. Ehrenberg, C. Roth, Carbon materials for the positive electrode in all-vanadium redox flow batteries, *Carbon* 78 (2014) 220–230, <https://doi.org/10.1016/j.carbon.2014.06.075>.
- [89] A. Di Blasi, O. Di Blasi, N. Briguglio, A.S. Arico, D. Sebastián, M.J. Lázaro, G. Monforte, V. Antonucci, Investigation of several graphite-based electrodes for vanadium redox flow cell, *J. Power Sources* 227 (2013) 15–23, <https://doi.org/10.1016/j.jpowsour.2012.10.098>.
- [90] B. Sun, M. Skyllas-Kazacos, Chemical modification of graphite electrode materials for vanadium redox flow battery application—part II. Acid treatments, *Electrochim. Acta* 37 (1992) 2459–2465, [https://doi.org/10.1016/0013-4686\(92\)87084-D](https://doi.org/10.1016/0013-4686(92)87084-D).
- [91] L. Yue, W. Li, F. Sun, L. Zhao, L. Xing, Highly hydroxylated carbon fibres as electrode materials of all-vanadium redox flow battery, *Carbon* 48 (2010) 3079–3090, <https://doi.org/10.1016/j.carbon.2010.04.044>.
- [92] E. Agar, C.R. Dennison, K.W. Knehr, E.C. Kumbur, Identification of performance limiting electrode using asymmetric cell configuration in vanadium redox flow batteries, *J. Power Sources* 225 (2013) 89–94, <https://doi.org/10.1016/j.jpowsour.2012.10.016>.
- [93] B. Sun, M. Skyllas-Kazacos, Modification of graphite electrode materials for vanadium redox flow battery application—I. Thermal treatment, *Electrochim. Acta* 37 (1992) 1253–1260, [https://doi.org/10.1016/0013-4686\(92\)85064-R](https://doi.org/10.1016/0013-4686(92)85064-R).
- [94] C. Flox, M. Skoumal, J. Rubio-Garcia, T. Andreu, J.R. Morante, Strategies for enhancing electrochemical activity of carbon-based electrodes for all-vanadium redox flow batteries, *Appl. Energy* 109 (2013) 344–351, <https://doi.org/10.1016/j.apenergy.2013.02.001>.
- [95] S. Rümmler, M. Steimecke, S. Schimpf, M. Hartmann, S. Förster, M. Bron, Highly graphitic, mesoporous carbon materials as electrocatalysts for vanadium redox reactions in all-vanadium redox-flow batteries, *J. Electrochem. Soc.* 165 (2018) A2510–A2518, <https://doi.org/10.1149/2.1251810jes>.
- [100] Q. Ma, C. Mao, L. Zhao, Z. Chen, H. Su, Q. Xu, A pore-scale study for reactive transport processes in double-layer gradient electrode as negative side of a deep eutectic solvent electrolyte-based vanadium-iron redox flow battery, *Electrochim. Acta* 431 (2022) 141110, <https://doi.org/10.1016/j.electacta.2022.141110>.
- [101] M. Balakrishnan, P. Shrestha, N. Ge, C. Lee, K.F. Fahy, R. Zeis, V.P. Schulz, B. D. Hatton, A. Bazylak, Designing tailored gas diffusion layers with pore size gradients via electrospinning for polymer electrolyte membrane fuel cells, *ACS Appl. Energy Mater.* 3 (2020) 2695–2707, <https://doi.org/10.1021/acsaem.9b02371>.
- [102] H.R. Jiang, B.W. Zhang, J. Sun, X.Z. Fan, W. Shyy, T.S. Zhao, A gradient porous electrode with balanced transport properties and active surface areas for vanadium redox flow batteries, *J. Power Sources* 440 (2019) 227159, <https://doi.org/10.1016/j.jpowsour.2019.227159>.
- [103] Q. Ma, W. Fu, L. Zhao, Z. Chen, H. Su, Q. Xu, A double-layer electrode for the negative side of deep eutectic solvent electrolyte-based vanadium-iron redox flow battery, *Energy* 265 (2023) 126291, <https://doi.org/10.1016/j.energy.2022.126291>.
- [104] Q. Wu, Y. Lv, L. Lin, X. Zhang, Y. Liu, X. Zhou, An improved thin-film electrode for vanadium redox flow batteries enabled by a dual layered structure, *J. Power Sources* 410–411 (2019) 152–161, <https://doi.org/10.1016/j.jpowsour.2018.11.020>.
- [105] C. Yao, H. Zhang, T. Liu, X. Li, Z. Liu, Cell architecture upswing based on catalyst coated membrane (CCM) for vanadium flow battery, *J. Power Sources* 237 (2013) 19–25, <https://doi.org/10.1016/j.jpowsour.2013.03.014>.
- [106] X.L. Zhou, Y.K. Zeng, X.B. Zhu, L. Wei, T.S. Zhao, A high-performance dual-scale porous electrode for vanadium redox flow batteries, *J. Power Sources* 325 (2016) 329–336, <https://doi.org/10.1016/j.jpowsour.2016.06.048>.
- [107] X.L. Zhou, T.S. Zhao, Y.K. Zeng, L. An, L. Wei, A highly permeable and enhanced surface area carbon-cloth electrode for vanadium redox flow batteries, *J. Power Sources* 329 (2016) 247–254, <https://doi.org/10.1016/j.jpowsour.2016.08.085>.
- [108] R. Wang, M. Hao, C. He, Z. Tu, F. Chong, Y. Li, Gradient-distributed NiCo<sub>2</sub>O<sub>4</sub> nanorod electrode for redox flow batteries: establishing the ordered reaction interface to meet the anisotropic mass transport, *Appl. Catal. B Environ.* 332 (2023) 122773, <https://doi.org/10.1016/j.apcatb.2023.122773>.
- [109] W. Xing, S.Z. Qiao, R.G. Ding, F. Li, G.Q. Lu, Z.F. Yan, H.M. Cheng, Superior electric double layer capacitors using ordered mesoporous carbons, *Carbon* 44 (2006) 216–224, <https://doi.org/10.1016/j.carbon.2005.07.029>.
- [110] D.-W. Wang, F. Li, M. Liu, G.Q. Lu, H.-M. Cheng, 3D aperiodic hierarchical porous graphitic carbon material for high-rate electrochemical capacitive energy storage, *Angew. Chem. Int. Edit.* 47 (2008) 373–376, <https://doi.org/10.1002/anie.200702721>.
- [111] C. Flox, C. Fàbrega, T. Andreu, A. Morata, M. Skoumal, J. Rubio-Garcia, J. R. Morante, Highly electrocatalytic flexible nanofiber for improved vanadium-based redox flow battery cathode electrodes, *RSC Adv.* 3 (2013) 12056, <https://doi.org/10.1039/c3ra40463c>.
- [112] J. Sun, H.R. Jiang, M.C. Wu, X.Z. Fan, C.Y.H. Chao, T.S. Zhao, Aligned hierarchical electrodes for high-performance aqueous redox flow battery, *Appl. Energy* 271 (2020) 115235, <https://doi.org/10.1016/j.apenergy.2020.115235>.
- [113] J. Sun, M.C. Wu, X.Z. Fan, Y.H. Wan, C.Y.H. Chao, T.S. Zhao, Aligned microfibers interweaved with highly porous carbon nanofibers: a novel electrode for high-power vanadium redox flow batteries, *Energy Storage Mater.* 43 (2021) 30–41, <https://doi.org/10.1016/j.ensm.2021.08.034>.
- [114] J.L. Erkal, A. Selimovic, B.C. Gross, S.Y. Lockwood, E.L. Walton, S. McNamara, R. S. Martin, D.M. Spence, 3D printed microfluidic devices with integrated versatile and reusable electrodes, *Lab Chip* 14 (2014) 2023–2032, <https://doi.org/10.1039/C4LC00171K>.
- [115] W. Yu, H. Zhou, B.Q. Li, S. Ding, 3D printing of carbon nanotubes-based microsupercapacitors, *ACS Appl. Mater. Interfaces* 9 (2017) 4597–4604, <https://doi.org/10.1021/acsaami.6b13904>.
- [116] X. Wang, M. Jiang, Z. Zhou, J. Gou, D. Hui, 3D printing of polymer matrix composites: a review and prospective, *Compos. B Eng.* 110 (2017) 442–458, <https://doi.org/10.1016/j.compositesb.2016.11.034>.
- [117] S.D. Lacey, D.J. Kirsch, Y. Li, J.T. Morgenstern, B.C. Zarket, Y. Yao, J. Dai, L. Q. Garcia, B. Liu, T. Gao, S. Xu, S.R. Raghavan, J.W. Connell, Y. Lin, L. Hu, Extrusion-based 3D printing of hierarchically porous advanced battery electrodes, *Adv. Mater.* 30 (2018) 1705651, <https://doi.org/10.1002/adma.201705651>.
- [118] W. Hao, Y. Liu, H. Zhou, H. Chen, D. Fang, Preparation and characterization of 3D printed continuous carbon fiber reinforced thermosetting composites, *Polym. Test.* 65 (2018) 29–34, <https://doi.org/10.1016/j.polymtest.2017.11.004>.
- [119] K. Fu, Y. Yao, J. Dai, L. Hu, Progress in 3D printing of carbon materials for energy-related applications, *Adv. Mater.* 29 (2017) 1603486, <https://doi.org/10.1002/adma.201603486>.
- [120] N. Li, Y. Li, S. Liu, Rapid prototyping of continuous carbon fiber reinforced polyactic acid composites by 3D printing, *J. Mater. Process. Technol.* 238 (2016) 218–225, <https://doi.org/10.1016/j.jmatprotec.2016.07.025>.
- [121] X. Tian, T. Liu, Q. Wang, A. Dilmurat, D. Li, G. Ziegmann, Recycling and remanufacturing of 3D printed continuous carbon fiber reinforced PLA composites, *J. Clean. Prod.* 142 (2017) 1609–1618, <https://doi.org/10.1016/j.jclepro.2016.11.139>.
- [122] S. Mubarak, D. Dhamodharan, H.-S. Byun, Recent advances in 3D printed electrode materials for electrochemical energy storage devices, *J. Energy Chem.* 81 (2023) 272–312, <https://doi.org/10.1016/j.jechem.2023.01.037>.
- [123] J. Sun, M. Wu, H. Jiang, X. Fan, T. Zhao, Advances in the design and fabrication of high-performance flow battery electrodes for renewable energy storage, *Adv. Appl. Energy* 2 (2021) 100016, <https://doi.org/10.1016/j.adapen.2021.100016>.
- [124] S. Tsushima, T. Suzuki, Modeling and simulation of vanadium redox flow battery with interdigitated flow field for optimizing electrode architecture, *J. Electrochem. Soc.* 167 (2020) 020553, <https://doi.org/10.1149/1945-7111/ab6dd0>.
- [125] M. Liu, J. Waugh, S.K. Babu, J.S. Spendelow, Q. Kang, Numerical modeling of ion transport and adsorption in porous media: a pore-scale study for capacitive deionization desalination, *Desalination* 526 (2022) 115520, <https://doi.org/10.1016/j.desal.2021.115520>.
- [126] M.D.R. Kok, A. Khalifa, J.T. Gostick, Multiphysics simulation of the flow battery cathode: cell architecture and electrode optimization, *J. Electrochem. Soc.* 163 (2016) A1408–A1419, <https://doi.org/10.1149/2.1281607jes>.
- [127] X. Wang, B. Ding, J. Yu, M. Wang, F. Pan, A highly sensitive humidity sensor based on a nanofibrous membrane coated quartz crystal microbalance, *Nanotechnology* 21 (2009) 055502, <https://doi.org/10.1088/0957-4484/21/5/055502>.
- [128] Z. Li, W. Kang, H. Zhao, M. Hu, N. Wei, J. Qiu, B. Cheng, A novel polyvinylidene fluoride tree-like nanofiber membrane for microfiltration, *Nanomaterials* 6 (2016) 152, <https://doi.org/10.3390/nano6080152>.
- [129] A.-Y. Jiang, Z.-J. Pan, Surface-porous and hollow poly(lactic acid) (SPH-PLA) and surface-porous and lotus-root-like PLA (SPL-PLA) nanofibres: preparation, quantitative analysis, and modelling, *J. Nanopart. Res.* 22 (2020) 239, <https://doi.org/10.1007/s11051-020-04965-w>.
- [130] Z. Wei, J. Gu, F. Zhang, Z. Pan, Y. Zhao, Core-shell structured nanofibers for lithium ion battery separator with wide shutdown temperature window and stable electrochemical performance, *ACS Appl. Polym. Mater.* 2 (2020) 1989–1996, <https://doi.org/10.1021/acsaem.0c00164>.
- [131] R. Liao, H. Wang, W. Zhang, J. Shi, M. Huang, Z. Shi, W. Wei, X. Li, S. Liu, High-rate sodium storage performance enabled using hollow Co<sub>3</sub>O<sub>4</sub> nanoparticles anchored in porous carbon nanofibers anode, *J. Alloys Compd.* 868 (2021) 159262, <https://doi.org/10.1016/j.jallcom.2021.159262>.
- [132] F. Topuz, T. Uyar, Electrospinning of gelatin with tunable fiber morphology from round to flat/ribbon, *Mater. Sci. Eng. C* 80 (2017) 371–378, <https://doi.org/10.1016/j.msec.2017.06.001>.
- [133] J. Zhu, C. Yan, G. Li, H. Cheng, Y. Li, T. Liu, Q. Mao, H. Cho, Q. Gao, C. Gao, M. Jiang, X. Dong, X. Zhang, Recent developments of electrospun nanofibers for

- electrochemical energy storage and conversion, *Energy Storage Mater.* 65 (2024) 103111, <https://doi.org/10.1016/j.ensm.2023.103111>.
- [134] W.-Y. Hsieh, C.-H. Leu, C.-H. Wu, Y.-S. Chen, Measurement of local current density of all-vanadium redox flow batteries, *J. Power Sources* 271 (2014) 245–251, <https://doi.org/10.1016/j.jpowsour.2014.06.081>.
- [136] Q. Liu, A. Turhan, T.A. Zawodzinski, M.M. Mench, In situ potential distribution measurement in an all-vanadium flow battery, *Chem. Commun.* 49 (2013) 6292–6294, <https://doi.org/10.1039/C3CC42092B>.
- [137] M. Becker, N. Bredemeyer, N. Tenhumberg, T. Turek, Polarization curve measurements combined with potential probe sensing for determining current density distribution in vanadium redox-flow batteries, *J. Power Sources* 307 (2016) 826–833, <https://doi.org/10.1016/j.jpowsour.2016.01.011>.
- [138] J. Houser, J. Clement, A. Pezeshki, M.M. Mench, Influence of architecture and material properties on vanadium redox flow battery performance, *J. Power Sources* 302 (2016) 369–377, <https://doi.org/10.1016/j.jpowsour.2015.09.095>.
- [139] A.A. Wong, S.M. Rubinstein, M.J. Aziz, Direct visualization of electrochemical reactions and heterogeneous transport within porous electrodes in operando by fluorescence microscopy, *Cell Rep. Phys. Sci.* 2 (2021) 100388, <https://doi.org/10.1016/j.xcrp.2021.100388>.
- [140] J. Rubio-Garcia, A. Kucernak, A. Charleson, Direct visualization of reactant transport in forced convection electrochemical cells and its application to redox flow batteries, *Electrochem. Commun.* 93 (2018) 128–132, <https://doi.org/10.1016/j.elecom.2018.07.002>.
- [141] A.A. Wong, M.J. Aziz, S. Rubinstein, Direct visualization of electrochemical reactions and comparison of commercial carbon papers *in operando* by fluorescence microscopy using a quinone-based flow cell, *ECS Trans.* 77 (2017) 153–161, <https://doi.org/10.1149/07711.0153ecst>.
- [142] F. Tariq, J. Rubio-Garcia, V. Yufit, A. Bertei, B.K. Chakrabarti, A. Kucernak, N. Brandon, Uncovering the mechanisms of electrolyte permeation in porous electrodes for redox flow batteries through real time in situ 3D imaging, *Sustain. Energy Fuels* 2 (2018) 2068–2080, <https://doi.org/10.1039/C8SE00174J>.
- [143] K. Köble, L. Eifert, N. Bevilacqua, K.F. Fahy, A. Bazylak, R. Zeis, Synchrotron X-ray radiography of vanadium redox flow batteries – time and spatial resolved electrolyte flow in porous carbon electrodes, *J. Power Sources* 492 (2021) 229660, <https://doi.org/10.1016/j.jpowsour.2021.229660>.
- [144] D. Zhang, A. Forner-Cuenca, O.O. Taiwo, V. Yufit, F.R. Brushett, N.P. Brandon, S. Gu, Q. Cai, Understanding the role of the porous electrode microstructure in redox flow battery performance using an experimentally validated 3D pore-scale lattice Boltzmann model, *J. Power Sources* 447 (2020) 227249, <https://doi.org/10.1016/j.jpowsour.2019.227249>.